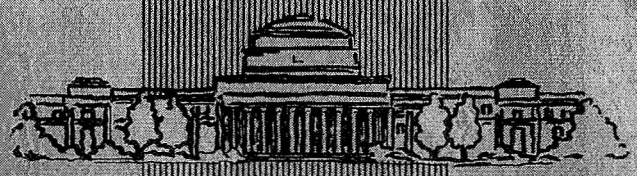

MASSACHUSETTS INSTITUTE OF TECHNOLOGY

RE-59

UNCERTAINTY ESTIMATION VIA PREFLIGHT TEST PROCEDURES FOR A SPACE STABILIZED INERTIAL NAVIGATION SYSTEM

by

NGR-22-009-229

Henry K. Johansen

MEASUREMENT SYSTEMS LABORATORY

MASSACHUSETTS INSTITUTE OF TECHNOLOGY
CAMBRIDGE 39, MASSACHUSETTS

RE-59

UNCERTAINTY ESTIMATION VIA PREFLIGHT TEST PROCEDURES FOR A *SPACE STABILIZED INERTIAL NAVIGATION SYSTEM*

by

NGR-22-009-229

Henry K. Johansen

August, 1969

Approved: W. C. Mackey

Director
Measurement Systems Laboratory

Abstract

A space stabilized inertial navigation system is used in VTOL aircraft where flight times of a maximum of one and a half hours duration is expected. This report deals with the usefulness of a preflight test run on a stationary base lasting less than 20 minutes in estimating the I.N.S. uncertainties. The use of data from the alignment phase is also discussed. A simple estimation procedure not including any optimal filtering techniques is assumed. The error propagation for a maximum one and a half hour run is derived when compensation signals with and without a succeeding realignment of the platform is applied.

Acknowledgements

This report was prepared under DSR Project No. 70343 sponsored by the National Aeronautics and Space Administration Electronic Research Center, Cambridge, Massachusetts, through NASA Grant No. NGR 22-009-229.

The publication of this report does not constitute approval by the National Aeronautics and Space Administration or by the MIT Measurement Systems Laboratory of the findings or the conclusions contained therein. It is published only for the exchange and stimulation of ideas.

Table of Contents

List of Symbols

Indices used most

a	The actual instrument frame.
a'	Ideal instrument frame. Coincides with the n frame at t = 0.
a_o	Actual instrument frame at t = 0.
c	Constant.
e	Reference ellipsoid of the earth or frame rotating with the earth.
i	Non-rotating frame with the origin at the center of the earth and the z axis along the earth axis.
m	Measured value.
r	Random.
$()_n$	Value after compensation.
$()_p$	Value in the preflight test run.
(1)	System 1 using a theodolite in aligning azimuth.
(2)	System 2, gyrocompassing.

Symbols used most

(Number in parentheses denotes the equation in which the quantity is given.)

$\underline{A}^a$	Accelerometer scale factor uncertainty matrix, (3.14).
$\underline{A}_1$	Uncertainty matrix, (4.3a).
a_k, k = x,y,z	Terms of $\underline{A}^a$.
$\underline{B}$	Transformation matrix given by (3.5).
$\underline{C}^a$	Platform misalignment found from the steady state solution, (2.11), (2.16).
$\underline{C}'^a$	Platform misalignment when the navigation phase commences, (2.18b, c).
$\underline{C}^a_{a_o}$	Transformation matrix transforming a vector specified in the a_o frame to the a frame, (3.6).
$\underline{C}^{a_o}_{a'}$	(2.17)

Symbols used most (continued)

$\underline{C}_i^{a'}$	(3.2)
$\underline{C}_n^a$	(2.4)
$\underline{C}_n^{a'}$	(3.1), (3.4)
$\underline{C}_{a'}^i$	(3.20a)
$\underline{C}_n^i$	(3.3)
$\hat{\underline{C}}_a^i$	Estimated transformation matrix, (3.20).
$\underline{D}^a$	Drift angle matrix, (3.7).
d_k, k = x,y,z	Terms of $\underline{D}^a$, (3.13).
$\underline{E}$, $\underline{E}_i$, i = 1,2,3,4	Estimation error matrix, (5.10b), (4.8a, b, c), (5.15a).
F(0)	DC gain in the leveling loops for system 1.
$\underline{f}_m^a$	Measured accelerometer outputs, (3.17), (3.19).
$\underline{f}^n$	Specific force coordinatized in the n frame, (2.8).
$\underline{G}_c^i$	Computed gravitation, (3.21).
$\underline{g}_e^n$	Gravity for the reference ellipsoid, (2.8a).
$\underline{K}_i$, i = 1 to 11	Uncertainty matrices, (3.25a) to (3.25k).
L_o	Latitude for the stationary vehicle.
$p = \frac{d}{dt}$	Time derivative.
r_o	Distance from the center of the earth to the vehicle.
T	Length of preflight test run.
$\underline{U}_i$, i = 2 to 5	Uncertainty matrices, (3.29, b, c, d, e).
$\underline{U}_i'$, i = 2 to 5	Residual uncertainty matrices after compensation.
$\hat{\underline{U}}_2$, $\hat{\underline{U}}_3$	Estimated uncertainty matrices, (4.9a, b).
(u)$\ddot{\underline{r}}$	Disturbing accelerations, (2.8).
(u)ψ	Misalignment of the theodolite.
$\underline{Z}^a$	Computation uncertainty matrix, (3.20).
$\underline{\alpha}^n$	Deflection of the vertical matrix, (2.8b).

Symbols used most (continued)

$\underline{\Delta f}^a$	Error in measured specific force, (4.4).
ΔV	Velocity increment from accelerometers.
$\underline{\delta f}^a$	Accelerometer bias, (2.2).
δg	Error in estimating gravity.
$\underline{\delta r}^{a'}$, $\underline{\delta r}^i$	Error in computer position.
$\underline{\delta r}(0)^i$	Error in initial position, (3.22).
$\underline{\delta V}(0)^i$	Error in initial velocity, (3.23).
$\underline{\varepsilon}_{ik}$	Element of $\underline{E}_i$.
$\underline{\varepsilon r}(T)^{a'}$	(5.8b)
$\underline{\dot{\varepsilon r}}(T)^{a'}$	(5.8c)
$\underline{\zeta}_c^a$	Misalignment due to offsets in the alignment electronics, (2.11a), (2.15a).
ζ_k, ζ'_z $k = x,y,z$	Misalignment terms, (2.17d).
ζ_{rk}, $k = x,y,z$	Misalignment terms varying from alignment to alignment, (2.17d).
η, ξ	Elements of $\underline{\alpha}^n$.
$\underline{\psi}^a$	Misalignment matrix, (2.17), (2.18).
ψ_f^a, ψ_α^a, ψ_ω^a, ψ_u^a	Misalignment matrix, (2.17a, b, c, d).
$\underline{\omega}_{do}^a$	Total gyro drift when platform is level, (2.1), (3.12), (3.13).
ω_{ie}	Earth rate referred to initial space.
ω_s	Schuler frequency, paragraph 3.2.2.
∂f_k, $l = x,y$	Change in bias, (3.18).

1. INTRODUCTION

A space stabilized inertial navigation system is considered for use on a VTOL aircraft. Prior to takeoff, the platform is aligned and the INS uncertainties estimated and compensated for by using data from the alignment phase or from a short test run lasting less than 20 minutes.

The platform is physically leveled to the local vertical in the alignment phase by means of standard leveling loops using the x and y accelerometers on the platform as sensors. In azimuth two different concepts are considered. System 1 uses an optical alignment scheme with a ground based theodolite. A signal proportional to the misalignment between the x axis of the inner member of the platform and north is fed to the azimuth gyro torquer through a proper transfer function, thereby physically aligning the platform to north. In System 2 the platform is aligned to north by use of a simple gyrocompassing scheme. When the alignment phase is finished, the system is switched to the navigation mode. The computation is performed in an earth centered inertial frame (the analysis is also valid for a tangential inertial frame). During a 10-20 minute test run on a stationary base, the position error and indicated acceleration error are monitored or used simultaneously to compute the various uncertainties. Compensation signals are then established and applied to the system when the test run is finished together with a possible realignment of the platform. The estimation procedure assumed could be a least squares fitting method.

The error propagation for a one and a half hour run after compensation is derived for four different compensation schemes, one incorporating a realignment of the platform and one using only data from the alignment phase.

A stationary base assumption is made and the uncertainties taken into consideration are:

- Acceleration insensitive- and acceleration-sensitive gyro drift
- Accelerometer bias and scale factor uncertainties
- Misalignment uncertainties
- Initial latitude and altitude error
- Initial velocity error
- Deflection of the vertical
- Imperfections in the electronics

All the uncertainties are regarded as constants during a run and some are allowed to vary from alignment to alignment.

2. ALIGNMENT ERRORS

The alignment errors caused by the inertial instruments depend upon the alignment scheme used. The two methods treated here use accelerometers to physically level the platform. In System 1 a theodolite is used to align the azimuth gimbal with north; in System 2 a simple gyrocompassing scheme is used. The alignment is performed while the vehicle is at rest.

2.1 Theodolite Alignment of Azimuth

Figure 2.1 shows a simplified functional block diagram for System 1.

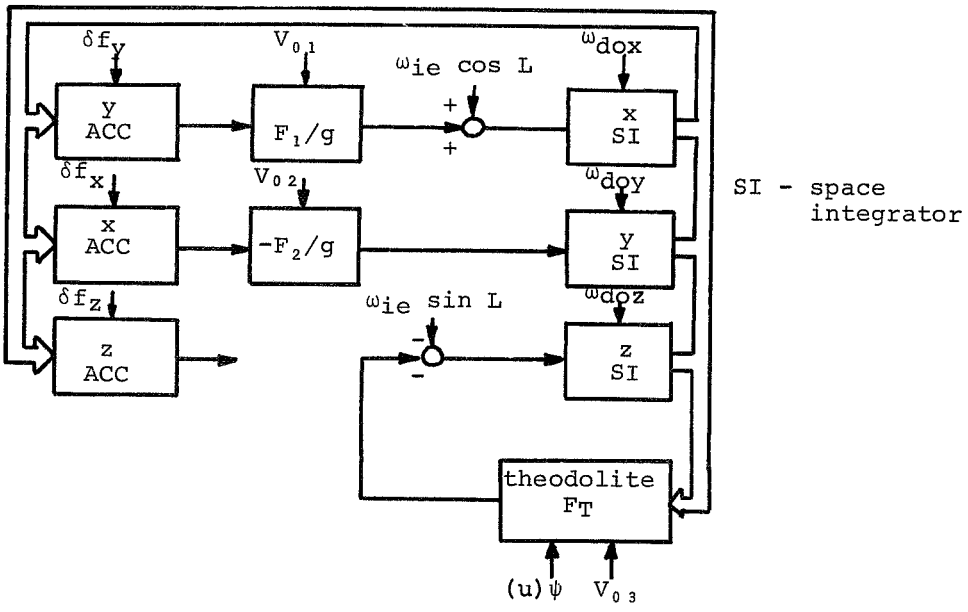

Figure 2.1
Functional Block Diagram for Alignment, System 1

During the alignment mode the instrument frame, x, y, z, is brought in alignment with the geographic frame, north, east, and down, respectively.

The transfer functions F_1, F_2, and F_T can be shaped as a low pass filter to reduce the effect of disturbing accelerations. At lower frequencies they can also be configured as integrators to reduce the effect of gyro drift.

The uncertainties taken into consideration are:

$\underline{\omega}^a_{do} = \{\omega_{dox}, \omega_{doy}, \omega_{doz}\}$ - the total gyro drift rates when the platform is level (2.1)

$\underline{\delta f}^a = \{\delta f_x, \delta f_y, \delta f_z\}$ - accelerometer bias (2.2)

$(u)\psi$ - uncertainty in the alignment of the theodolite with north

$\underline{V}^a_o = \{V_{01}, V_{02}, V_{03}\}$ - constant offsets in the alignment electronics

The accelerometer scale factor uncertainties can be neglected in these servoloops.

Assuming that the small angle approximation is valid, the following equations will describe the alignment mode:

Forced rate of turn of control member

$$\underline{\omega}^a_{ia} = \underline{\omega}^a_{CMD(1)} + \underline{\omega}^a_{do} \tag{2.3a}$$

which equals

$$\underline{\omega}^a_{ia} = \underline{C}^a_n \, \underline{\omega}^n_{in} + \underline{\omega}^a_{na} \tag{2.3b}$$

where

$\omega_{CMD(1)}$ - command rate for System 1

index a - instrument frame

index n - geographic frame, north, east, and down

index i - earth centered frame, non-rotating with respect to inertial space, z_i-axis along the earth axis

$\underline{C}^a_n$ - transformation from n-frame to a-frame

$\underline{\omega}^n_{in}$ - rotation of n-frame with respect to i-frame coordinatized in the n-frame

The alignment error matrix is

$$\underline{C}_n^a = \begin{bmatrix} 1 & C_z & -C_y \\ -C_z & 1 & C_x \\ C_y & -C_x & 1 \end{bmatrix} \tag{2.4}$$

where C_x is the positive rotation about the x_a-axis (or x_n-axis), etc.

The change in the error angles between a-frame and n-frame is:

$$\underline{\omega}_{na}^a = \begin{bmatrix} p & C_x \\ p & C_y \\ p & C_z \end{bmatrix} \tag{2.5}$$

where $p = \frac{d}{dt}$

and the inertial angular velocity of the n-frame is given by:

$$\underline{\omega}_{in}^n = \begin{bmatrix} \omega_{ie} \cos L_o \\ 0 \\ -\omega_{ie} \sin L_o \end{bmatrix} \tag{2.6}$$

where ω_{ie} is the earth rate and L_o is the latitude.

The command rate to the space integrator is (Ref. Figure 2.1)

$$\underline{\omega}_{CMD(1)}^a = \begin{bmatrix} 0 & F_1/g & 0 \\ -F_2/g & 0 & 0 \\ 0 & 0 & 0 \end{bmatrix} (\underline{C}_n^a \underline{f}^n + \underline{\delta f}^a + \underline{V}_o^a) + \begin{bmatrix} \omega_{ie} \cos L_o \\ 0 \\ -\omega_{ie} \sin L_o - F_T(C_z\text{-}(u)\psi - V_{03}) \end{bmatrix} \tag{2.7}$$

The specific force can be expressed as

$$\underline{f}^n = -\underline{g}_e^n - \underline{\alpha}^n + (u)\underline{\ddot{r}} \tag{2.8}$$

where

$$\underline{g}_e^n = \begin{bmatrix} 0 \\ 0 \\ g \end{bmatrix} \quad \text{Gravity computed for the reference ellipsoid} \tag{2.8a}$$

$$\underline{\alpha}^n = \begin{bmatrix} \xi g \\ -\eta g \\ 0 \end{bmatrix} \quad \text{Deflection of the vertical} \tag{2.8b}$$

where η, ξ = the positive rotations about the north and east axes, respectively, and $(u)\underline{\ddot{r}}$ = the acceleration disturbances with no DC components.

By combining equations (2.1) through (2.8), neglecting products of uncertainties, we get

$$\begin{bmatrix} (p + F_1) & \omega_{ie} \sin L_o & 0 \\ -\omega_{ie} \sin L_o & (p + F_2) & -\omega_{ie} \cos L_o \\ 0 & \omega_{ie} \cos L_o & (p + F_T) \end{bmatrix} \begin{bmatrix} C_x \\ C_y \\ C_z \end{bmatrix} = \begin{bmatrix} F_1(\delta f_y/g + \eta + V_{01}/g + (u)\ddot{r}_y/g) + \omega_{dox} \\ -F_2(\delta f_x/g - \xi + V_{02}/g + (u)\ddot{r}_x/g) + \omega_{doy} \\ F_T((u)\psi + V_{03}) + \omega_{doz} \end{bmatrix} \tag{2.9}$$

Provided that we have a non-oscillatory system, the stationary values of the alignment errors can be found. Assuming constant values of the uncertainties and adequate damping of the $u(\ddot{r})$ terms, we can write:

$$\begin{bmatrix} F_1(0) & \omega_{ie} \sin L_o & 0 \\ -\omega_{ie} \sin L_o & F_2(0) & -\omega_{ie} \cos L_o \\ 0 & \omega_{ie} \cos L_o & F_T(0) \end{bmatrix} \begin{bmatrix} C_x \\ C_y \\ C_z \end{bmatrix}_{\text{steady state}} = \begin{bmatrix} F_1(0)(\delta f_y/g + \eta + V_{01}/g) + \omega_{dox} \\ -F_2(0)(\delta f_x/g - \xi + V_{02}/g) + \omega_{doy} \\ F_T(0)((u)\psi + V_{03}) + \omega_{doz} \end{bmatrix} \tag{2.10}$$

where F(0) denotes the DC gain of the respective transfer functions.

From (2.10) it is evident that by choosing $F_1(0)$, $F_2(0)$, and $F_T(0) >> \omega_{ie}$, the cross coupling terms can be neglected. Choosing $F_1(0) = F_2(0) = F(0)$, equation (2.10) can be simplified to:

$$\underline{C}^a = \begin{bmatrix} C_x \\ C_y \\ C_z \end{bmatrix} = \begin{bmatrix} (\delta f_y/g + \eta) + \zeta_{cx} + \omega_{dox}/F(0) \\ -(\delta f_x/g - \xi) + \zeta_{cy} + \omega_{doy}/F(0) \\ (u)\psi + \zeta_{cz} + \omega_{doz}/F_T(0) \end{bmatrix} \tag{2.11}$$

where

$$\underline{\zeta}_c^a = \{\zeta_{cx}, \zeta_{cy}, \zeta_{cz}\} = \{V_{01}/g, -V_{02}/g, V_{03}\} \qquad (2.11a)$$

is the misalignment caused by offsets in the alignment electronics. In most well designed systems F(0) and $F_T(0)$ are large. E.g. for F(0) formed as a low pass filter with a 10 second time constant, a well damped loop gives approximately 2 μrad misalignment per 1 meru gyro drift, giving a ratio of F(0) to ω_{ie} of 500:1.

2.2 Alignment Using Gyrocompassing

A simplified functional block diagram for System 2, where simple physical gyrocompassing is applied, is shown in Figure 2.2.

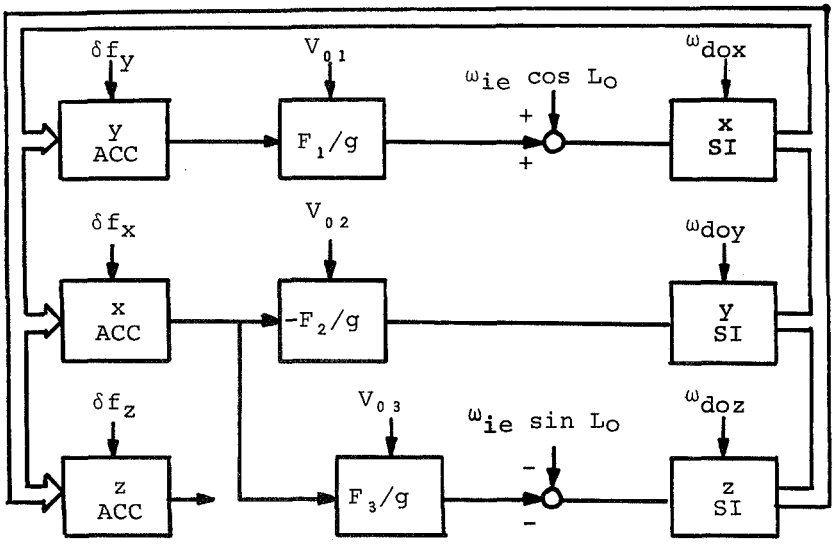

Figure 2.2
Functional Block Diagram of System 2

In deriving the equations for this system, the same comments as for System 1 are valid. The command rates fed to the space integrators are:

$$\underline{\omega}^{a}_{CMD(2)} = \begin{bmatrix} 0 & F_1/g & 0 \\ -F_2/g & 0 & 0 \\ -F_3/g & 0 & 0 \end{bmatrix} (\underline{C}^{a}_{n}\,\underline{f}^{n} + \underline{\delta f}^{a} + \underline{V}^{a}_{o}) \begin{bmatrix} \omega_{ie}\cos L_o \\ 0 \\ -\omega_{ie}\sin L_o \end{bmatrix} \tag{2.12}$$

By combining equations (2.1) through (2.6), (2.8a,b) and (2.12), the result is:

$$\begin{bmatrix} (p + F_1) & \omega_{ie}\sin L_o & 0 \\ -\omega_{ie}\sin L_o & (p + F_2) & -\omega_{ie}\cos L_o \\ 0 & F_3 + \omega_{ie}\cos L_o & p \end{bmatrix} \begin{bmatrix} C_x \\ C_y \\ C_z \end{bmatrix} = \begin{bmatrix} F_1(\delta f_y/g + \eta + V_{01}/g + (u)\ddot{r}_y/g) + \omega_{dox} \\ -F_2(\delta f_x/g - \xi + V_{02}/g + (u)\ddot{r}_x/g) + \omega_{doy} \\ -F_3(\delta f_x/g - \xi + V_{03}/g + (u)\ddot{r}_x/g) + \omega_{doz} \end{bmatrix} \tag{2.13}$$

Assuming stable alignment loops and constant uncertainties, the steady state angular errors are given by:

$$\begin{bmatrix} F_1(0) & \omega_{ie}\sin L_o & 0 \\ -\omega_{ie}\sin L_o & F_2(0) & -\omega_{ie}\cos L_o \\ 0 & F_3(0) + \omega_{ie}\cos L_o & 0 \end{bmatrix} \begin{bmatrix} C_x \\ C_y \\ C_z \end{bmatrix}_{\substack{\text{steady} \\ \text{state}}} = \begin{bmatrix} F_1(0)\left(\frac{\delta f_y}{g} + \eta + \frac{V_{01}}{g}\right) + \omega_{dox} \\ -F_2(0)\left(\frac{\delta f_x}{g} - \xi + \frac{V_{02}}{g}\right) + \omega_{doy} \\ -F_3(0)\left(\frac{\delta f_x}{g} - \xi + \frac{V_{03}}{g}\right) + \omega_{doz} \end{bmatrix} \tag{2.14}$$

F_1, F_2, and F_3 are assumed to perform an effective filtering of the acceleration disturbances.

Choosing $F_1(0)$ and $F_2(0) >> \omega_{ie}$, we get

$$\begin{bmatrix} C_x \\ C_y \\ C_z \end{bmatrix}_{\substack{\text{steady} \\ \text{state}}} = \begin{bmatrix} (\delta f_y/g + \eta) + \zeta_{cx} + \omega_{dox}/F_1(0) \\ -(\delta f_x/g - \xi) + \zeta_{cy} + \omega_{doz}/F_3(0) \\ -(\delta f_y/g + \eta + \zeta_{cx}) \tan L_o - \dfrac{\omega_{doy}}{\omega_{ie}\cos L_o} - \dfrac{\omega_{dox}}{F_1(0)} \tan L_o + \\ + \dfrac{F_2(0)\ \omega_{doz}}{F_3(0)\omega_{ie}\cos L_o} + \dfrac{F_2(0)}{F_3(0)} \left(\dfrac{\delta f_x}{g} - \xi - \zeta_{cy}\right) + \zeta_{cz} \end{bmatrix} \tag{2.15}$$

where

$$\underline{\zeta}_c^a = \{\zeta_{cx},\ \zeta_{cy}, \zeta_{cz}\} = \frac{1}{g}\{V_{01},\ -V_{03},\ \frac{F_2(0)}{\omega_{ie}\cos L_o}(V_{02} - V_{03})\} \tag{2.15a}$$

By making $F_1(0)$, $F_2(0)$, and $F_3(0)$ large or, even better, by designing F_1 and F_3 as a proportional plus integral filter and F_2 as a low pass filter, equation (2.15) simplifies to:

$$\underline{C}^a = \begin{bmatrix} C_x \\ C_y \\ C_z \end{bmatrix}_{\substack{\text{steady} \\ \text{state}}} = \begin{bmatrix} \delta f_y/g + \eta + \zeta_{cx} \\ -(\delta f_x/g - \xi) + \zeta_{cy} \\ -(\delta f_y/g + \eta + \zeta_{cx}) \tan L_o - \dfrac{\omega_{doy}}{\omega_{ie}\cos L_o} + \zeta_{cz} \end{bmatrix} \tag{2.16}$$

2.3 The Alignment Uncertainty Matrix

An alignment uncertainty matrix valid for the two alignment schemes described in parts 2.1 and 2.2 can be written by using equations (2.3), (2.11), and (2.16):

$$\underline{C}_{a'}^{a_o} = \underline{I} + \underline{\psi}^a = \underline{I} + \underline{\psi}_f^a + \underline{\psi}_\alpha^a + \underline{\psi}_\omega^a + \underline{\psi}_u^a \tag{2.17}$$

where the $\underline{C}_{a'}^{a_o}$ denotes a transformation from the a'-frame, which coincides with the n-frame at t = 0, to the a-frame at t = 0. The system is switched from the alignment mode to the navigation mode at t = 0.

$\underline{\psi}_f^a$ is a skew symmetric matrix associated with alignment errors due to accelerometer bias.

$$\underline{\psi}_f^a = \begin{bmatrix} 0 & \psi_{fz} & \delta f_x/g \\ -\psi_{fz} & 0 & \delta f_y/g \\ -\delta f_x/g & -\delta f_y/g & 0 \end{bmatrix} \tag{2.17a}$$

where:

$$\psi_{fz(1)} = (u)\psi$$

$$\psi_{fz(2)} = -\frac{f_y}{g} \tan L_o$$

Subscript (1) - theodolite alignment of azimuth
Subscript (2) - gyrocompassing

$\underset{\sim}{\psi}_{\alpha}^{a}$ is a matrix associated with misalignment caused by the deflection of the vertical.

$$\underset{\sim}{\psi}_{\alpha}^{a} = \begin{bmatrix} 0 & \psi_{\alpha z} & -\xi \\ -\psi_{\alpha z} & 0 & \eta \\ \xi & -\eta & 0 \end{bmatrix} \tag{2.17b}$$

where:

$$\psi_{\alpha z(1)} = 0$$

$$\psi_{\alpha z(2)} = -\eta \tan L_o$$

$\underset{\sim}{\psi}_{\omega}^{a}$ denotes a matrix associated with misalignment due to the effect of gyro drift rates during alignment.

$$\underset{\sim}{\psi}_{\omega}^{a} = \begin{bmatrix} 0 & \psi_{\omega z} & -\psi_{\omega y} \\ -\psi_{\omega z} & 0 & \psi_{\omega x} \\ \psi_{\omega y} & -\psi_{\omega x} & 0 \end{bmatrix} \tag{2.17c}$$

where:

$$\begin{bmatrix} \psi_{\omega x} \\ \psi_{\omega y} \\ \psi_{\omega z} \end{bmatrix}_{(1)} = \begin{bmatrix} \omega_{dox}/F(0) \\ \omega_{doy}/F(0) \\ \omega_{doz}/F_T(0) \end{bmatrix}$$

and

$$\begin{bmatrix} \psi_{\omega x} \\ \psi_{\omega y} \\ \psi_{\omega z} \end{bmatrix}_{(2)} = \begin{bmatrix} 0 \\ 0 \\ -\dfrac{\omega_{doy}}{\omega_{ie} \cos L_o} \end{bmatrix}$$

$\underline{\psi}_u^a$ is a skew symmetric matrix associated with a misalignment caused by offsets in the alignment electronics and effects not included in the analysis in paragraphs 2.1 and 2.2. These misalignments give rise to steady state accelerometer signals.

$$\underline{\psi}_u^a = \begin{bmatrix} 0 & \zeta'_z & -\zeta_y \\ -\zeta'_z & 0 & \zeta_x \\ \zeta_y & -\zeta_x & 0 \end{bmatrix} \qquad (2.17d)$$

where

$$\zeta'_{z(1)} = \zeta_z, \quad \zeta'_{z(2)} = \zeta_z - \zeta_x \tan L_o$$

and

$$\underline{\zeta}^a = \underline{\zeta}_c^a + \underline{\zeta}_r^a$$

and

$\underline{\zeta}_c^a$ is given by the equations (2.11a) for system 1 and (2.15a) for system 2 and is caused by constant offsets in the alignment electronics.

$\underline{\zeta}_r^a = \{\zeta_{rx}, \zeta_{ry}, \zeta_{rz}\}$ This unpredictable alignment error can be caused by:

a) Limit cycles in the alignment loops which can give unknown alignment errors when the system is switched to the navigation mode.

b) Transients which have not died out when the navigation mode commences.

c) Electrical transients in the gyro torquer electronics which can arise when the system is switched to the navigation mode. The effect appears as a step in the misalignment angle.

It can also be convenient to express the $\underline{\psi}^a$ matrix in equation (2.17) as:

$$\underline{\psi}^a = \begin{bmatrix} 0 & C'_z & -C'_y \\ -C'_z & 0 & C'_x \\ C'_y & -C'_x & 0 \end{bmatrix} \tag{2.18}$$

where the C'_k, $k = x, y, z$, denote the misalignment just after switching to the navigation mode

$$\underline{C}'^a = \underline{C}^a + \underline{\zeta}_r^a \tag{2.18a}$$

$\underline{C}^a$ misalignment derived from the steady state analysis, equations (2.11) and (2.16), and $\underline{\zeta}_r^a$ is given connection with (2.17d)

or:

$$\begin{bmatrix} C'_x \\ C'_y \\ C'_z \end{bmatrix} = \begin{bmatrix} \delta f_y/g + \eta + \psi_{\omega x} + \zeta_x \\ -(\delta f_x/g - \xi) + \psi_{\omega y} + \zeta_y \\ \psi_{fz} + \psi_{\alpha z} + \psi_{\omega z} + \zeta'_z \end{bmatrix} \tag{2.18b}$$

Using the definitions given in connection with (2.17a, b, c, d), this becomes:

$$\begin{bmatrix} C'_x \\ C'_y \\ C'_z \end{bmatrix} = \begin{bmatrix} \delta f_y/g + \eta + \zeta_x \\ -(\delta f_x/g - \xi) + \zeta_y \\ \zeta_z \end{bmatrix} + \begin{bmatrix} \omega_{dox}/F(0) \\ \omega_{doy}/F(0) \\ (u)\psi + \omega_{doy}/F(0) \end{bmatrix}_{(1)} + \begin{bmatrix} 0 \\ 0 \\ -(\delta f_y/g + \eta + \zeta_x) \tan L_o - \dfrac{\omega_{doy}}{\omega_{ie} \cos L_o} \end{bmatrix}_{(2)} \tag{2.18c}$$

3. EVALUATION OF SYSTEM EQUATIONS FOR THE NAVIGATION MODE

In the navigation mode the IMU is space stabilized, i.e., only gyro drift compensation signals are applied to the gyro torquers. The navigation mode starts when the system is switched from the alignment mode ($t = 0$). The IMU is then ideally aligned physically with the geographical frame.

Figure 3.1 shows the signal flow diagram for this system:

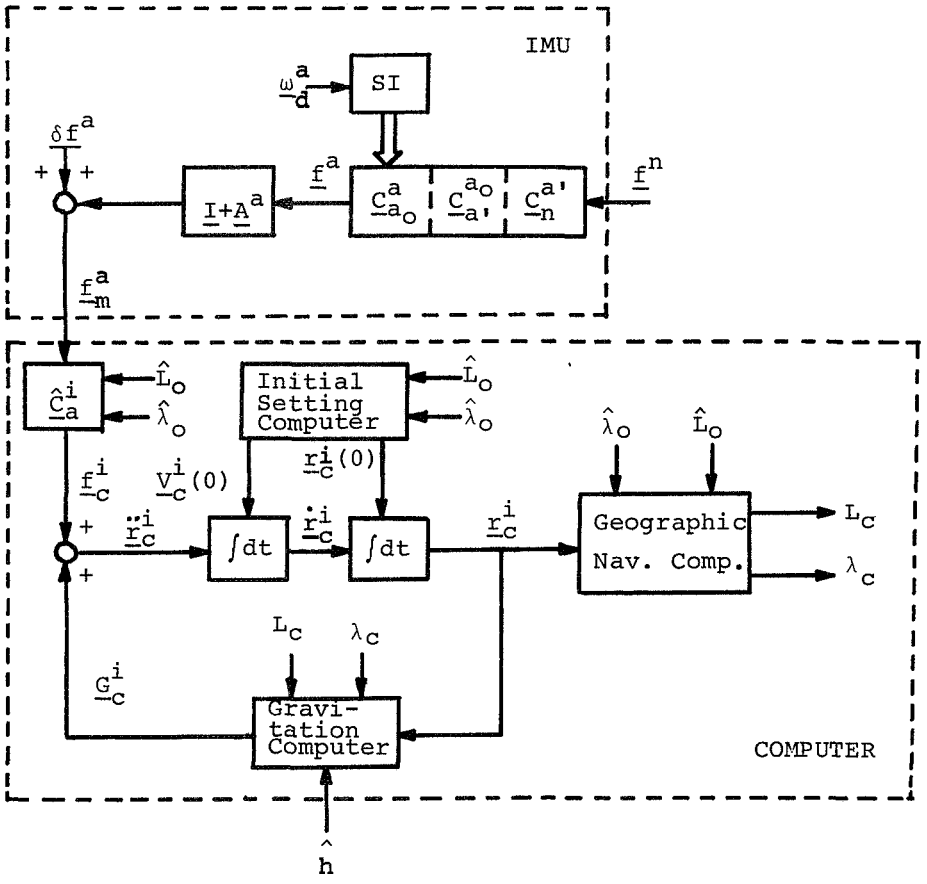

Figure 3.1
Signal Flow Diagram for the Navigation Mode

The quantities involved in figure 3.1 are:

$\underline{C}_n^{a'}$ Matrix transforming specific force from the actual geographic frame to the ideal instrument frame which coincides with the n-frame at t = 0.

$\underline{C}^{a_o}_{a'}$ This matrix transforms the specific force from the ideal instrument frame to the actual instrument frame at t = 0. This transformation is caused by physical misalignment of the IMU.

$\underline{C}^{a}_{a_o}$ This transformation is due to the drift of the space integrator, SI, for t > 0 and is caused by gyro drift.

$\hat{\underline{C}}^{i}_{a}$ Estimated transformation matrix stored in the computer for transforming the measured specific force to the earth centered inertial frame where the computation is performed.

$\underline{A}^{a}$ Accelerometer scale factor uncertainties.

$\underline{\delta f}^{a}$ Accelerometer bias.

$\underline{f}^{a}_{m}$ Specific force measured by the accelerometers.

Subscript m Denotes a quantity actually measured.

Subscript c Denotes a quantity computed by the navigation computer.

Hat (^) Denotes an estimated quantity fed into the computer.

3.1 The IMU Outputs

The only quantities from the IMU used by the computer is the output from the accelerometers. In the proceeding paragraphs, the expressions for the matrices involved will be derived.

3.1.1 The $\underline{C}^{a'}_{n}$ Matrix

We have

$$\underline{C}^{a'}_{n} = \underline{C}^{a'}_{i}\ \underline{C}^{i}_{n} \tag{3.1}$$

where $\underline{C}^{a'}_{i}$ is a constant matrix dependent only upon the alignment location. This location is given by

L_o, ℓ_o - Actual latitude and longitude where alignment was performed. Without loss of generality, ℓ_o can be set to zero (i.e., y_n - and y_i axis parallel).

Then

$$\underline{C}_i^{a'} = \begin{bmatrix} -\sin L_o & 0 & \cos L_o \\ 0 & 1 & 0 \\ -\cos L_o & 0 & -\sin L_o \end{bmatrix} \tag{3.2}$$

Further, we have

$$\underline{C}_n^i = \begin{bmatrix} -\sin L \cos \lambda & -\sin \lambda & -\cos L \cos \lambda \\ -\sin L \sin \lambda & \cos \lambda & -\cos L \sin \lambda \\ \cos L & 0 & -\sin L \end{bmatrix} \tag{3.3}$$

where

$$L = L_o$$

$$\lambda = \omega_{ie} t \quad \text{This is true only if } \ell = \ell_o$$

and the vehicle is at rest.

Equations (3.1), (3.2) and (3.3) then give:

$$\underline{C}_n^{a'} = \underline{I} + \underline{B} \tag{3.4}$$

where:

$$\underline{B} = -\begin{bmatrix} (1-\cos \omega_{ie} t)\sin^2 L_o & -\sin \omega_{ie} t \sin L_o & (1-\cos \omega_{ie} t) \sin L_o \cos L_o \\ \sin \omega_{ie} t \sin L_o & 1-\cos \omega_{ie} t & \sin \omega_{ie} t \cos L_o \\ (1-\cos \omega_{ie} t) \sin L_o \cos L_o & -\sin \omega_{ie} t \cos L_o & (1-\cos \omega_{ie} t)\cos^2 L_o \end{bmatrix} \tag{3.5}$$

This matrix vanishes when $t = 0$.

3.1.2 Gyro Uncertainties

The value of the $\underline{C}_{a_o}^a$ matrix depends upon the drift of the three gyros of the space integrator. Because the drift angles are small, we can write:

$$\underline{C}_{a_o}^a = \underline{I} + \underline{D}^a \tag{3.6}$$

$$\underline{D}^a = \begin{bmatrix} 0 & d_z & -d_y \\ -d_z & 0 & d_x \\ d_y & -d_x & 0 \end{bmatrix} \tag{3.7}$$

where d_k, k = x, y, z can be associated with the drift angle k about the positive instrument frame axis k caused by the k^{th} gyro during the navigation mode.

Gyro Drift Model

In this analysis only the main gyro drift sources such as acceleration-insensitive drift rate (AI) and acceleration-sensitive drift rate due to mass unbalance in the gyro (AS) are taken into account. These drift rates are regarded as constant for a time period up to one and a half hours, a realistic maximum flight time for VTOL aircraft.

The AI drift rate can be written as:

$$\underline{\omega}^a_{AI} = \begin{bmatrix} \omega_{AI_x} \\ \omega_{AI_y} \\ \omega_{AI_z} \end{bmatrix} \tag{3.8}$$

and the AS drift rate as:

$$\underline{\omega}^a_{AS} = \underline{MU}\ \underline{f}^a \tag{3.9}$$

where the $\underline{MU}$, the mass unbalance matrix, can be written as:

$$\underline{MU} = \begin{bmatrix} MUX_x & MUY_x & MUZ_x \\ MUX_y & MUY_y & MUZ_y \\ MUX_z & MUY_z & MUZ_z \end{bmatrix} \tag{3.10}$$

where MUX_y denotes the mass unbalance drift rate of the y gyro caused by acceleration along the x axis. When the actual orientation of the gyros is known, the elements of $\underline{MU}$ will be the MUI, MUS, and MUO ($\approx$0) drift rates for the three gyros. (Note that MUK_k, k = x, y, z equals plus or minus MUI_k)

The total gyro drift rate can then be expressed as:

$$\underline{\omega}^a_d = \underline{\omega}^a_{AI} + \underline{\omega}^a_{AS}$$

or

$$\underline{\omega}_d^a = \underline{\omega}_{do}^a + \underline{\Delta\omega}_{AS}^a \tag{3.11}$$

where

$$\underline{\omega}_{do}^a = \underline{\omega}_{AI}^a + \underline{\omega}_{AS}^a(t = 0), \text{ the total gyro drift for a level platform}$$

$$\underline{\Delta\omega}_{AS}^a = \underline{\omega}_{AS}^a - \underline{\omega}_{AS}^a(t = 0)$$

$$\underline{\Delta\omega}_{AS}^a(t = 0) = 0$$

Expression (3.11) is useful when the gyro drift rates are determined by not rotating the instrument frame with respect to the n-frame. For a space stabilized platform, the $\underline{\Delta\omega}_{AS}$ is of importance because of the rotations of the platform with respect to the earth, while it can be neglected when the instrument frame is aligned with the geographical frame, provided that the effect of the accelerations of the vehicle can be neglected compared with the effect of the gravity.

By neglecting the effect of the acceleration of the vehicle, equation (3.9) can be written as:

$$\underline{\omega}_{AS}^a = \underline{\underline{MU}}\ \underline{\underline{C}}_n^a\ \underline{f}^n \approx -\underline{\underline{MU}}\ \underline{\underline{C}}_n^a\ \underline{g}_e^n \approx -\underline{\underline{MU}}\ \underline{\underline{C}}_n^{a'}\ \underline{g}_e^n$$

when higher order error terms are neglected.

This gives:

$$\underline{\omega}_{AS}^a(t = 0) = -\underline{\underline{MU}}\ \underline{g}_e^n = -g \begin{bmatrix} MUZ_x \\ MUZ_y \\ MUZ_z \end{bmatrix}$$

and

$$\underline{\omega}_{do}^a = \begin{bmatrix} \omega_{dox} \\ \omega_{doy} \\ \omega_{doz} \end{bmatrix} = \begin{bmatrix} \omega_{AI_x} - g\ MUZ_x \\ \omega_{AI_y} - g\ MUZ_y \\ \omega_{AI_z} - g\ MUZ_z \end{bmatrix} \tag{3.12}$$

Using equation (3.4) the time varying drift term becomes:

$$\underline{\Delta\omega}^a_{AS} = -\underline{MU}(\underline{C}_n^{a'} - \underline{I})\underline{g}_e^n = -\underline{MU}\ \underline{B}\ \underline{g}_e^n$$

The drift angle d_k can now be found by integrating equation (3.11):

$$d_k = \int_o^t \omega_{dk}(\tau)d\tau \qquad k = x, y, z$$

$$\int_o^t \underline{\omega}^a_d(\tau)d\tau = \int_o^t \underline{\omega}^a_{do}d\tau + \int_o^t \underline{\Delta\omega}^a_{AS}(\tau)d\tau$$

$$= \underline{\omega}^a_{do}t - \underline{MU}(\int_o^t \underline{B}(\tau)d\tau)\underline{g}_e^n$$

Using equation (3.5) for $\underline{B}$ this results in:

$$\begin{bmatrix} d_x \\ d_y \\ d_z \end{bmatrix} = \begin{bmatrix} \omega_{dox} \\ \omega_{doy} \\ \omega_{doz} \end{bmatrix} t + \frac{g}{\omega_{ie}} \begin{bmatrix} MUY_x \\ MUY_y \\ MUY_z \end{bmatrix} (1-\cos\ \omega_{ie}t) + \frac{1}{\omega_{ie}} \begin{bmatrix} \omega_{MU_x} \\ \omega_{MU_y} \\ \omega_{MU_z} \end{bmatrix} (\omega_{ie}t-\sin\ \omega_{ie}t) \tag{3.13}$$

where

$$\begin{bmatrix} \omega_{MU_x} \\ \omega_{MU_y} \\ \omega_{MU_z} \end{bmatrix} = g \begin{bmatrix} MUX_x \sin L_o \cos L_o + MUZ_x \cos^2 L_o \\ MUX_y \sin L_o \cos L_o + MUZ_y \cos^2 L_o \\ MUX_z \sin L_o \cos L_o + MUZ_z \cos^2 L_o \end{bmatrix} \tag{3.13a}$$

Equation (3.13) gives the terms of the $\underline{D}^a$ matrix, equation (3.7).

3.1.3 Accelerometer Uncertainties

The accelerometer uncertainties taken into consideration during the navigation mode are scale factor uncertainties, $\underline{A}^a$, and bias uncertainties, $\underline{\delta f}^a$, which can be regarded constant for at least one and a half hours.

$$\underline{A}^a = \begin{bmatrix} a_x & 0 & 0 \\ 0 & a_y & 0 \\ 0 & 0 & a_z \end{bmatrix} \tag{3.14}$$

$$\underline{\delta f}^a = \begin{bmatrix} \delta f_x \\ \delta f_y \\ \delta f_z \end{bmatrix} \tag{3.15}$$

The bias terms are not necessarily the same during the alignment phase and the navigation phase.

3.1.4 Measured Specific Force

From Figure 3.1 the output from the accelerometers is given by:

$$\underline{f}_m^a = (\underline{I} + \underline{A}^a)\, C_{a_o}^a\, \underline{C}_{a'}^{a_o}\, \underline{C}_n^{a'}\, \underline{f}^n + \underline{\delta f}^a \tag{3.16}$$

Using equations (2.17) and (3.6), equation (3.16) can then be written as:

$$\underline{f}_m^a = (\underline{I} + \underline{A}^a)(\underline{I} + \underline{D}^a)(\underline{I} + \underline{\psi}^a)\underline{C}_n^{a'}\underline{f}^n + \underline{\delta f}^a$$

By neglecting products of uncertainties, after inserting equation (2.8) this becomes:

$$\underline{f}_m^a = \underline{C}_n^{a'}\underline{f}^n - (\underline{A}^a + \underline{D}^a + \underline{\psi}_f^a + \underline{\psi}_\alpha^a + \underline{\psi}_\omega^a + \underline{\psi}_u^a)\underline{C}_n^{a'}\underline{g}_e^n + \underline{\delta f}^a$$

or when (3.4) is used:

$$\begin{aligned} \underline{f}_m^a = {} & \underline{C}_n^{a'}\underline{f}^n + \underline{\alpha}^n + \underline{\partial f}^a - (\underline{\psi}_f^a + \underline{\psi}_\alpha^a)\underline{B}\underline{g}_e^n - \\ & (\underline{A}^a + \underline{D}^a + \underline{\psi}_\omega^a + \underline{\psi}_u^a)\underline{C}_n^{a'}\underline{g}_e^n \end{aligned} \tag{3.17}$$

where:

$$\underline{\alpha}^n = -\underline{\psi}_\alpha^a\, \underline{g}_e^n = \begin{bmatrix} \xi g \\ -\eta g \\ 0 \end{bmatrix}$$

derived from equations (2.8a, b) and (2.17b), and

$$\underline{\partial f}^a = \underline{\delta f}^a - \underline{\psi}_f^a\, \underline{g}_e^n = \underbrace{\begin{bmatrix} \delta f_x \\ \delta f_y \\ \delta f_z \end{bmatrix}}_{t \geq 0} - \underbrace{\begin{bmatrix} \delta f_x \\ \delta f_y \\ 0 \end{bmatrix}}_{t < 0} = \begin{bmatrix} \partial f_x \\ \partial f_y \\ \delta f_z \end{bmatrix} \tag{3.18}$$

This equation is derived from equations (3.15) for $t \geq 0$, (2.17a) and (2.8a), valid for the alignment phase.

The ∂f_x and ∂f_y terms can be caused by a sudden change in the ground potential or an electrical offset is removed by disconnecting the alignment electronics when the system is switched to the navigation mode. This results in a steplike change in the signals from the accelerometers which is not caused by a shift in platform attitude or in specific force.

Equation (3.17) can also be written as:

$$\underline{f}_m^a = +\underline{C}_n^{a'}(-\underline{g}_e^n + (u)\ddot{\underline{r}}) + \underline{\partial f}^a - \underline{B\alpha}^n - (\underline{\psi}_f^a + \underline{\psi}_\alpha^a)\underline{B}\underline{g}_e^n - (\underline{A}^a + \underline{D}^a + \underline{\psi}_\omega^a + \underline{\psi}_u^a)\underline{C}_n^{a'}\underline{g}_e^n \tag{3.19}$$

Equation (3.19) shows that in the beginning of the navigation mode while the $\underline{C}_n^{a'} \approx \underline{I}$ and $\underline{B} \approx \underline{0}$, the constant bias of the x and y accelerometers and the deflection of the vertical are not traceable in the accelerometer outputs. This is due to the fact that the leveling loops seek to null the accelerometer outputs during the alignment mode, resulting in a tilt of the platform which gives an effective compensation for the bias terms and the deflection of the vertical when the specific force consists mainly of the gravity.

3.2 The Navigation Computation

The navigation computer does the computation of the velocity and position in the earth centered inertial frame. The different terms involved in the computation are derived in the proceeding paragraphs.

3.2.1 The $\hat{\underline{C}}_a^i$ Matrix

Ideally, one wants to insert into the computer a matrix transforming the specific force measured in the a frame to the i frame. Because the a frame differs from the desired a' frame due to unknown uncertainties in the IMU, the best we can do is to use the constant $\hat{\underline{C}}_a^i$, matrix. This matrix can be estimated by using the estimated values of the latitude and longitude, $\hat{L}_o$ and $\hat{\lambda}$.

$$\hat{\underline{C}}_a^i = \begin{bmatrix} -\sin\hat{L}_o\cos\hat{\lambda}_o & -\sin\hat{\lambda}_o & -\cos\hat{L}_o\cos\hat{\lambda}_o \\ -\sin\hat{L}_o\sin\hat{\lambda}_o & \cos\hat{\lambda}_o & -\cos\hat{L}_o\sin\hat{\lambda}_o \\ \cos\hat{L}_o & 0 & -\sin\hat{L}_o \end{bmatrix}$$

Now

$$\hat{L}_o = L_o + \delta L_o$$

where L_o is the true value and δL_o is the error in the estimate of L_o.

$$\hat{\lambda}_o = 0$$

i.e., the x axis of the i frame is defined to intersect with the actual meridian through the vehicle. The error in $\hat{\lambda}_o$ has importance for the set value of the latitude-longitude computer only.

We then get:

$$\hat{\underline{C}}_a^i = \underline{C}_a^i \cdot (\underline{I} + \underline{Z}^a) \tag{3.20}$$

where

$$\underline{C}_{a'}^i = \begin{bmatrix} -\sin L_o & 0 & -\cos L_o \\ 0 & 1 & 0 \\ \cos L_o & 0 & -\sin L_o \end{bmatrix} \tag{3.20a}$$

and

$$\underline{Z}^a = \begin{bmatrix} 0 & 0 & -\delta L_o \\ 0 & 0 & 0 \\ \delta L_o & 0 & 0 \end{bmatrix} \tag{3.20b}$$

3.2.2 Computation of Gravitation

To get a stable computation of position, external altitude information is used together with the computed position to calculate the gravitation for the reference ellipsoid. The error in the computed gravitation can, after neglecting the second order error terms, be found using a model for a spherical earth.

$$\underline{G}_{cs}^i = -\frac{E\ \underline{r}_c^i}{(r_e + h)^3}$$

where

r_e - radius of the earth

h - altitude

$\underline{r}_c^i$ - computed position

Using

$$\underline{r}_c^i = \underline{r}^i + \underline{\delta r}^i$$

$$h = h_o + \delta h$$

we get the computed gravitation.

$$\underline{G}_c^i = \underline{G}_e^i - \omega_s^2 \, \underline{\delta r}^i + 3\omega_s^2 \, \delta h \, \frac{\underline{r}^i}{r_o}$$

where

$\omega_s^2 = \dfrac{E}{(r_e + h_o)^3}$, the square of the Schuler frequency.

$r_o = r_e + h_o$ - distance from center of the earth to the vehicle

$\underline{G}_e^i$ - the gravitation for the reference ellipsoid which has been substituted for the gravitation of a sphere

$\underline{\delta r}^i$ - error in computed position

δh - error in estimated altitude

The last term of the expression above can be modified by neglecting second order errors:

$$3 \, \omega_s^2 \, \delta h \, \frac{\underline{r}^i}{r_o} = 3\omega_s^2 \, \delta h \, \underline{C}_n^i \, \frac{\underline{r}^n}{r_o} \approx - 3\omega_s^2 \, \delta h \, \underline{C}_n^i \, \frac{1}{g} \, \underline{g}_e^n$$

$$= -\underline{C}_a^i, \, 3 \, \frac{\delta h}{r_o} \, C_n^{a'} \underline{g}_e^n$$

where it was noted that $\omega_s^2 = g/r_o$.

Including the deflection of the vertical, the true gravitation is given by:

$$\underline{G}^i = \underline{G}_e^i + \underline{C}_n^i \, \underline{\alpha}^n$$

Thus, the computed gravitation can then be expressed as:

$$\underline{G}_c^i = \underline{G}^i - \omega_s^2 \, \underline{\delta r}^i - \underline{C}_n^i \, \underline{\alpha}^n - \underline{C}_a^i, \, 3 \, \frac{\delta h}{r_o} \, \underline{C}_n^{a'} \, \underline{g}_e^n \qquad (3.21)$$

3.2.3 Initial Setting of the Integrators

Just prior to switching the INS to the navigation mode, the velocity and position integrators are set with the initial values of the velocity and position of the vehicle in the i frame.

Position Setting

Because the exact position of the vehicle is not known, we have:

$$\underline{r}_c(0)^i = \hat{\underline{C}}_n^i \, \hat{\underline{r}}(0)^n$$

where

$\hat{\underline{C}}_n^i = \hat{\underline{C}}_a^i = \underline{C}_a^i \cdot (\underline{I} + \underline{Z}^a)$ because the a' frame coincides with the n frame at t = 0 when setting occurs.

Since

$$\underline{r}_c(0)^i = \underline{r}(0)^i + \underline{\delta r}(0)^i ,$$

then

$$\hat{\underline{r}}(0)^n = \underline{r}(0)^n + \underline{\delta r}(0)^n$$

where $\underline{\delta r}(0)^n$ consists of altitude error and unpredicted movements of the vehicle, neglected here. Using these equations, we get by neglecting higher order error terms:

$$\underline{\delta r}(0)^i = \underline{C}_a^i \cdot (\underline{Z}^a \, \underline{r}(0)^n + \underline{\delta r}(0)^n)$$

$$\underline{\delta r}(0)^i \approx \underline{C}_a^i \cdot \left(\begin{bmatrix} 0 & 0 & -\delta L_o \\ 0 & 0 & 0 \\ \delta L_o & 0 & 0 \end{bmatrix} \begin{bmatrix} 0 \\ 0 \\ -r_o \end{bmatrix} + \begin{bmatrix} 0 \\ 0 \\ -\delta h \end{bmatrix} \right)$$

$$\underline{\delta r}(0)^i = \underline{C}_a^i \cdot \begin{bmatrix} r_o \, \delta L_o \\ 0 \\ -\delta h \end{bmatrix} = \underline{C}_a^i \cdot \underline{\delta r}(0)^{a'} \quad (3.22)$$

Velocity Setting

By taking the derivative of $\underline{r}^i = \underline{C}_n^i \, \underline{r}^n$ and using the law of Coriolis, we get

$$\underline{V}^i = \underline{C}_n^i \, [\underline{V}^n + \underline{\Omega}_{in}^n \, \underline{r}^n]$$

Using this equation to compute the velocity at t = 0, we get:

$$\underline{V}_c(0)^i = \hat{\underline{C}}_a^i \left[\underline{V}_c(0)^{a'} + \underline{\Omega}_{in}^n \, \underline{r}_c(0)^{a'}\right]$$

where

$$\underline{V}_c(0)^i = \underline{V}(0)^i + \underline{\delta V}(0)^i$$

$\underline{V}_c(0)^{a'} = \underline{0}$, $\underline{V}(0)^{a'} = -(u)\underline{V}^{a'}$ caused by wind gusts, loading, etc.

$\hat{\underline{\Omega}}_{in}^n = \underline{\Omega}_{in}^n + \Delta\underline{\Omega}_{in}^n$ caused by uncertainty in L. (ω_{ie} is assumed to be applied without error.)

$$\underline{\Omega}_{in}^n = \begin{bmatrix} 0 & \omega_{ie} \sin L_o & 0 \\ -\omega_{ie} \sin L_o & 0 & -\omega_{ie} \cos L_o \\ 0 & \omega_{ie} \cos L_o & 0 \end{bmatrix}$$

$$\underline{\Delta\Omega}_{in}^n = \begin{bmatrix} 0 & \omega_{ie}\, \delta L_o \cos L_o & 0 \\ -\omega_{ie}\, \delta L_o \cos L_o & 0 & \omega_{ie}\, \delta L_o \sin L_o \\ 0 & -\omega_{ie}\, \delta L_o \sin L_o & 0 \end{bmatrix}$$

$$\hat{\underline{C}}_a^i = \underline{C}_a^i, \, (\underline{I} + \underline{Z}^a)$$

$$\underline{r}_c(0)^{a'} = \underline{r}(0)^{a'} + \underline{\delta r}(0)^{a'}$$

Neglecting products of uncertainties, these equations, together with (3.22) and (3.20b), give:

$$\underline{\delta V}(0)^i = \underline{C}_a^i, \left[(u)\underline{V}^{a'} + \underline{\Omega}_{in}^n \, \underline{\delta r}(0)^{a'} + (\underline{\Delta\Omega}_{in}^n + \underline{Z}^a \underline{\Omega}_{in}^n) r(0)^{a'}\right]$$

or finally,

$$\underline{\delta V}(0)^i = \underline{C}_a^i, \underline{\delta V}(0)^{a'} = \underline{C}_a^i, \begin{bmatrix} (u)V_x \\ (u)V_y + 2r_o\, \delta L_o\, \omega_{ie} \sin L_o + \delta h\, \omega_{ie} \cos L_o \\ (u)V_z \end{bmatrix} \tag{3.23}$$

3.3 Position Error Equations

From Figure 3.1 we get

$$\ddot{\underline{r}}_c^i = \underline{G}_c^i + \hat{\underline{C}}_a^i \underline{f}_m^a$$

By expressing

$$\ddot{\underline{r}}_c^i = \ddot{\underline{r}}^i + \delta\ddot{\underline{r}}^i$$

and inserting equations (3.21), (3.20), and (3.17), we get:

$$\delta\ddot{\underline{r}}^i + \ddot{\underline{r}}^i = \underline{G}^i - \omega_s^2 \delta\underline{r}^i - \underline{C}_n^i \underline{\alpha}^n - \underline{C}_a^i, 3 \frac{\delta h_o}{r_o} \underline{C}_n^{a'} \underline{g}_e^n +$$

$$\underline{C}_a^i, (\underline{I} + \underline{Z}^a)\{\underline{C}_n^{a'} \underline{f}^n + \underline{\alpha}^n + \underline{\partial f}^a - (\underline{\psi}_f + \underline{\psi}_\alpha)\underline{B}\, \underline{g}_e^n -$$

$$(\underline{A}^a + \underline{D}^a + \underline{\psi}_\omega^a + \underline{\psi}_u^a)\underline{C}_n^{a'} \underline{g}_e^n\}$$

Neglecting products of uncertainties and noting that

$$\ddot{\underline{r}}^i = \underline{G}^i + \underline{C}_a^i, \underline{C}_n^{a'} \underline{f}^n \quad \text{and} \quad \omega_s^2 = g/r_o,$$

the above equation can be rewritten as:

$$\delta\ddot{\underline{r}}^i + \omega_s^2 \delta\underline{r}^i = \underline{C}_a^i, \{\underline{\partial f}^a - \underline{B}\, \underline{\alpha}^n - (\underline{\psi}_f + \underline{\psi}_\alpha)\underline{B}\, \underline{g}_e^n -$$

$$(\underline{Z}^a + \underline{A}^a + \underline{D}^a + \underline{\psi}_\omega^a + \underline{\psi}_u^a + 3 \frac{\delta h}{r_o} \underline{I})\underline{C}_n^{a'} \underline{g}_e^n\} \tag{3.24}$$

where it was noted that

$$-\underline{C}_n^i \underline{\alpha}^n - \underline{C}_a^i, \underline{\alpha}^n = -\underline{C}_a^i, (\underline{I} + \underline{B})\, \underline{\alpha}^n - \underline{C}_a^i, \underline{\alpha}^n = -\underline{B}\, \underline{\alpha}^n$$

Equation (3.24) can now be expressed as a function of time by inserting the various matrices derived in this chapter.

$$\delta\ddot{\underline{r}}^i + \omega_s^2 \delta\underline{r}^i = \underline{C}_a^i, g\{\underline{K}_1 + \underline{K}_2\, \omega_{ie} t + \underline{K}_3 \sin \omega_{ie} t$$

$$+ \underline{K}_4 (1 - \cos \omega_{ie} t) + \underline{K}_5\, \omega_{ie} t \sin \omega_{ie} t$$

$$+ \underline{K}_6\, \omega_{ie} t\, (1 - \cos \omega_{ie} t) + \underline{K}_7 (\omega_{ie} t - \sin \omega_{ie} t)$$

$$+ \underline{K}_8 \sin \omega_{ie} t\, (1 - \cos \omega_{ie} t) + \underline{K}_9 (1 - \cos \omega_{ie} t)^2 +$$

$$+ \underline{K}_{10} \sin \omega_{ie}t \, (\omega_{ie}t - \sin \omega_{ie}t) + \underline{K}_{11} \, (1 - \cos \omega_{ie}t) \, (\omega_{ie}t - \sin \omega_{ie}t) \tag{3.25}$$

where

$$\underline{K}_1 = \begin{bmatrix} \partial f_x/g \\ \partial f_y/g \\ \delta f_z/g - a_z \end{bmatrix} + \begin{bmatrix} \psi_{\omega y} \\ -\psi_{\omega x} \\ 0 \end{bmatrix} + \begin{bmatrix} \zeta_y \\ -\zeta_x \\ 0 \end{bmatrix} + \begin{bmatrix} \delta L_o \\ 0 \\ -3 \, \delta h/r_o \end{bmatrix} \tag{3.25a}$$

$$\underline{K}_2 = \frac{1}{\omega_{ie}} \begin{bmatrix} \omega_{doy} \\ -\omega_{dox} \\ 0 \end{bmatrix} \tag{3.25b}$$

$$\underline{K}_3 = \begin{bmatrix} \psi_{fz} \cos L_o \\ a_y \cos L_o \\ -\delta f_y/g \cos L_o \end{bmatrix} + \begin{bmatrix} \eta \sin L_o + \psi_{\alpha z} \cos L_o \\ \xi \sin L_o \\ 0 \end{bmatrix} + \begin{bmatrix} \psi_{\omega z} \cos L_o \\ 0 \\ -\psi_{\omega x} \cos L_o \end{bmatrix}$$

$$+ \begin{bmatrix} \zeta'_z \cos L_o \\ 0 \\ -\zeta_x \cos L_o \end{bmatrix} + \begin{bmatrix} 0 \\ 3 \, \delta h/r_o \cos L_o \\ 0 \end{bmatrix} \tag{3.25c}$$

$$\underline{K}_4 = \begin{bmatrix} \delta f_x/g \cos^2 L_o + a_x \sin L_o \cos L_o \\ \delta f_y/g \cos^2 L_o - \psi_{fz} \sin L_o \cos L_o \\ -\delta f_x/g \sin L_o \cos L_o + a_z \cos^2 L_o \end{bmatrix} + \frac{g}{\omega_{ie}} \begin{bmatrix} MUY_x \\ -MUY_x \\ 0 \end{bmatrix}$$

$$+ \begin{bmatrix} \xi(1-2\cos^2 L_o) \\ -\eta(1-\cos^2 L_o) - \psi_{\alpha z} \sin L_o \cos L_o \\ 2\xi \sin L_o \cos L_o \end{bmatrix} + \begin{bmatrix} -\psi_{\omega y} \cos^2 L_o \\ \psi_{\omega x} \cos^2 L_o - \psi_{\omega z} \sin L_o \cos L_o \\ \psi_{\omega y} \sin L_o \cos L_o \end{bmatrix}$$

$$+ \begin{bmatrix} -\zeta_y \cos^2 L_o \\ \zeta_x \cos^2 L_o - \zeta'_z \sin L_o \cos L_o \\ \zeta_y \sin L_o \cos L_o \end{bmatrix} + \begin{bmatrix} 3\delta h/r_o \sin L_o \cos L_o - \delta L_o \cos^2 L_o \\ 0 \\ 3\delta h/r_o \cos^2 L_o + \delta L_o \sin L_o \cos L_o \end{bmatrix} \tag{3.25d}$$

$$\underline{K}_5 = \frac{\cos L_o}{\omega_{ie}} \begin{bmatrix} \omega_{doz} \\ 0 \\ -\omega_{dox} \end{bmatrix} \tag{3.25e}$$

$$\underline{K}_6 = \frac{\cos L_o}{\omega_{ie}} \begin{bmatrix} -\omega_{doy} \cos L_o \\ \omega_{dox} \cos L_o - \omega_{doz} \sin L_o \\ \omega_{doy} \sin L_o \end{bmatrix} \tag{3.25f}$$

$$\underline{K}_7 = \frac{1}{\omega_{ie}} \begin{bmatrix} \omega_{MU_y} \\ -\omega_{MU_x} \\ 0 \end{bmatrix} \tag{3.25g}$$

$$\underline{K}_8 = \frac{g \cos L_o}{\omega_{ie}} \begin{bmatrix} MUY_z \\ 0 \\ -MUY_x \end{bmatrix} \tag{3.25h}$$

$$\underline{K}_9 = \frac{g \cos L_o}{\omega_{ie}} \begin{bmatrix} -MUY_y \cos L_o \\ MUY_x \cos L_o - MUY_z \sin L_o \\ MUY_y \sin L_o \end{bmatrix} \tag{3.25i}$$

$$\underline{K}_{10} = \frac{\cos L_o}{\omega_{ie}} \begin{bmatrix} \omega_{MU_z} \\ 0 \\ -\omega_{MU_x} \end{bmatrix} \tag{3.25j}$$

$$\underline{K}_{11} = \frac{\cos L_o}{\omega_{ie}} \begin{bmatrix} -\omega_{MU_y} \cos L_o \\ \omega_{MU_x} \cos L_o - \omega_{MU_z} \sin L_o \\ \omega_{MU_y} \sin L_o \end{bmatrix} \tag{3.25k}$$

Solution of the Position Differential Equations

By assuming that the matrices $\underline{K}_1$ to $\underline{K}_{11}$ consist only of constant terms, i.e. gyro drifts and accelerometer uncertainties are time invariant, equation (3.25) can easily be solved by use of the Laplace transformation method. Using the initial conditions given by equations (3.22) and (3.23) we get:

$$
\begin{aligned}
\underline{\delta r}(s)^i = \underline{C}_{a'}^{i} \frac{g}{s^2+\omega_s^2} \{ & \underline{\delta r}(0)^{a'} s + \underline{\delta V}(0)^{a'} \\
& + \underline{K}_1 \frac{1}{s} + \underline{K}_2 \omega_{ie} \frac{1}{s^2} + \underline{K}_3 \frac{\omega_{ie}}{s^2+\omega_{ie}^2} \\
& + \underline{K}_4 \frac{\omega_{ie}^2}{s(s^2+\omega_{ie}^2)} + \underline{K}_5 \frac{2\omega_{ie} s}{(s^2+\omega_{ie}^2)^2} \\
& + \underline{K}_6 \omega_{ie} \left[\frac{1}{s^2} - \frac{s^2-\omega_{ie}^2}{(s^2+\omega_{ie}^2)^2} \right] + \underline{K}_7 \frac{\omega_{ie}^3}{s^2(s^2+\omega_{ie}^2)} \\
& + \underline{K}_8 \left[\frac{\omega_{ie}}{s^2+\omega_{ie}^2} - \frac{\omega_{ie}}{(s^2+4\omega_{ie}^2)} \right] \\
& + \underline{K}_9 \left[\frac{2\omega_{ie}^2}{s(s^2+\omega_{ie}^2)} - \frac{2\omega_{ie}^2}{s(s^2+4\omega_{ie}^2)(s^2+\omega_s^2)} \right] \\
& + \underline{K}_{10} \left[\frac{2\omega_{ie} s}{(s^2+\omega_{ie}^2)^2} - \frac{2\omega_{ie}^2}{s(s^2+4\omega_{ie}^2)} \right] \\
& + \underline{K}_{11} \left[\frac{\omega_{ie}}{s^2} - \frac{\omega_{ie}}{s^2+\omega_{ie}^2} - \frac{\omega_{ie}(s^2-\omega_{ie}^2)}{(s^2+\omega_{ie}^2)} + \frac{\omega_{ie}}{(s^2+\omega_{ie}^2)} \right] \Bigg\}
\end{aligned}
\tag{3.26}
$$

Transforming back to the time domain, (3.26) gives:

$$
\begin{aligned}
\underline{\delta r}^i = \underline{\delta r}(0)^i + \underline{C}_{a'}^{i} r_o \{ & [\frac{1}{r_o \omega_s} \underline{\delta V}(0)^{a'} - \frac{\omega_{ie}}{\omega_s}((1 + \frac{\omega_{ie}^2}{\omega_s^2} \underline{K}_3) + \underline{K}_2) \\
& + \frac{\omega_{ie}^3}{\omega_s^3} (3\underline{K}_6 + \underline{K}_7 + 3\underline{K}_8)] \sin \omega_s t +
\end{aligned}
$$

$$+ [(\underline{K}_1 - \frac{1}{r_o}\,\underline{\delta r}(0)^{a'}) - \frac{\omega_{ie}^2}{\omega_s^2}\,(\underline{K}_4 + 2\underline{K}_5)](1-\cos\,\omega_s t)$$

$$+ \underline{K}_2\,\omega_{ie}t + [\underline{K}_3(1 + \frac{\omega_{ie}^2}{\omega_s^2}) + \frac{\omega_{ie}^2}{\omega_s^2}\,(\underline{K}_6 - \underline{K}_7)]\,\sin\,\omega_{ie}t$$

$$+ [\underline{K}_4(1 + \frac{\omega_{ie}^2}{\omega_s^2}) + \frac{\omega_{ie}^2}{\omega_s^2}\,(2\underline{K}_5 + 2\underline{K}_{10})](1-\cos\,\omega_{ie}t)$$

$$+ \underline{K}_5(1 + \frac{\omega_{ie}^2}{\omega_s^2})\,\omega_{ie}t\,\sin\,\omega_{ie}t + \underline{K}_6(1 + \frac{\omega_{ie}^2}{\omega_s^2})\,\omega_{ie}\,(1-\cos\,\omega_{ie}t)$$

$$+ [\underline{K}_7 - \frac{\omega_{ie}^3}{\omega_s^3}\,\underline{K}_6](\omega_{ie}t - \sin\,\omega_{ie}t)$$

$$+ [\underline{K}_8\,(1 + \frac{\omega_{ie}^2}{\omega_s^2}) - 3\,\frac{\omega_{ie}^2}{\omega_s^2}\,\underline{K}_{11}]\,\sin\,\omega_{ie}t\,(1-\cos\,\omega_{ie}t)$$

$$+ \underline{K}_9\,(1 + \frac{\omega_{ie}^2}{\omega_s^2})(1-\cos\,\omega_{ie}t)^2 + \underline{K}_{10}(1 + \frac{\omega_{ie}^2}{\omega_s^2})\,\sin\,\omega_{ie}t$$

$$(\omega_{ie}t - \sin\,\omega_{ie}t)$$

$$+ \underline{K}_{11}(\omega_{ie}t - \sin\,\omega_{ie}t)(1-\cos\,\omega_{ie}t) + \underline{K}_{11}\,\frac{\omega_{ie}^2}{\omega_s^2}\,\cos\,\omega_{ie}t$$

$$(\omega_{ie}t - \sin\,\omega_{ie}t)$$

$$- \underline{K}_8\,\frac{3}{2}\,\frac{\omega_{ie}^2}{\omega_s^2}\,\sin\,2\omega_{ie}t - \frac{3}{2}\,\frac{\omega_{ie}^2}{\omega_s^2}\,(\underline{K}_9 + \underline{K}_{10})(1-\cos\,2\omega_{ie}t)\} \tag{3.27}$$

All terms multiplied by $(\frac{\omega_{ie}}{\omega_s})^n$, $n \geq 4$ have been neglected.

The coefficient of the $(1-\cos\,\omega_s t)$ term can be simplified using (3.25a) and (3.22) as:

$$(\underline{K}_1 - \frac{1}{r_o}\,\underline{\delta r}(0)^{a'}) = \begin{bmatrix} \partial f_x/g \\ \partial f_y/g \\ \delta f_z/g - a_z \end{bmatrix} + \begin{bmatrix} \psi_{\omega y} \\ -\psi_{\omega x} \\ 0 \end{bmatrix} + \begin{bmatrix} \zeta_y \\ -\zeta_x \\ 0 \end{bmatrix} + \begin{bmatrix} 0 \\ 0 \\ -2\,\frac{\delta h}{r_o} \end{bmatrix} \tag{3.27a}$$

where the initial latitude error is cancelled.

Equation (3.27) can be simplified because many of the terms will make an insignificant contribution to the position error. The following observations can be made:

All $(1 + \frac{\omega_{ie}^2}{\omega_s^2})$ factors can be reduced to 1 because this will introduce only 0.3% error in the estimate of the uncertainties.

The terms of the $\underline{K}$ matrices are normalized so that 1 meru, 1 mg, and 1 mrad give a factor of 10^{-3}.

It is more instructive to look at the position errors in the a' frame, which is the ideal instrument frame, than in the i frame. We can then substitute:

$$\underline{\delta r}^{a'} = \underline{C}_i^{a'} \underline{\delta r}^i$$

Excluding terms giving a contribution less than 130 feet propagating with the Schuler frequency and less than 1,000 feet after two hours propagating with the earth rate frequency when exposed to uncertainties with the following maximum values: 10 meru, 1 mg, 1 mrad, and 10^{-3}rad, equation (3.27) can be reduced to:

$$\begin{aligned}
\underline{\delta r}^{a'} = {} & \underline{\delta r}(0)^{a'} + r_o \{[\frac{1}{r_o \omega_s} \underline{\delta V}(0)^{a'} - \frac{\omega_{ie}}{\omega_s} (\underline{K}_2 + \underline{K}_3)] \sin \omega_s t \\
& + [(\underline{K}_1 - \frac{1}{r_o} \underline{\delta r}(0)^{a'}) - \frac{\omega_{ie}^2}{\omega_s^2} (\underline{K}_4 + 2\underline{K}_5)](1-\cos \omega_s t) \\
& + \underline{K}_2 \omega_{ie} t + \underline{K}_3 \sin \omega_{ie} t + \underline{K}_4 (1-\cos \omega_{ie} t) \\
& + \underline{K}_5 \omega_{ie} t \sin \omega_{ie} t + \underline{K}_6 \omega_{ie} t \, (1-\cos \omega_{ie} t) \\
& + \underline{K}_7 \, (\omega_{ie} t - \sin \omega_{ie} t) + \underline{K}_8 \sin \omega_{ie} t \, (1-\cos \omega_{ie} t) \\
& + \underline{K}_9 \, (1-\cos \omega_{ie} t)^2 + \underline{K}_{10} \sin \omega_{ie} t \, (\omega_{ie} t - \sin \omega_{ie} t) \\
& + \underline{K}_{11} (\omega_{ie} t - \sin \omega_{ie} t)(1-\cos \omega_{ie} t)\}
\end{aligned} \tag{3.28}$$

Further simplifications can be made because some of the terms in the $\underline{K}$ matrices will give negligible position errors.

On a stationary base, the deflection of the vertical results in the following position error:

100 feet/$\widehat{\text{sec}}$ after 6 hours, at $L_o = 45°$

200 feet/$\widehat{\text{sec}}$ after 12 hours, corresponding to 2 n.m. for the largest abnormality known

For comparison, 1 meru gyro drift rate gives 10 n.m. error after 12 hours. Thus, the deflection of the vertical will be neglected in this analysis. For an INS on a moving base going through regions with different deflections, a larger error contribution is expected because the compensating effect the alignment gave for an INS on a stationary base is reduced or even contributes to a larger error. On a moving base the deflection of the vertical gives the same effect as a variation of the bias terms.

3.4 Position Error for a Run Lasting Less than One and a Half Hours

If the length of a run is restricted to a maximum of one and a half hours, we can make the following substitutions in equation (3.28):

$$\sin \omega_{ie}t = \omega_{ie}t - \frac{1}{6}\omega_{ie}^3 t^3$$

$$1 - \cos \omega_{ie}t = \frac{1}{2}\omega_{ie}^2 t^2$$

The t^4 terms are neglected because they give a maximum contribution of 1,000 feet to the position error for a 10 meru gyro drift rate during a one and a half hour run. Equation (3.28) becomes:

$$\begin{aligned}\underline{\delta r}^{a'} = {} & \underline{\delta r}(0)^{a'} + \frac{1}{\omega_s}\underline{\delta V}(0)^{a'} \sin \omega_s t \\ & + r_o \underline{U}_2(1 - \cos \omega_s t) \\ & + r_o \frac{\omega_{ie}}{\omega_s}\underline{U}_3(\omega_s t - \sin \omega_s t) \\ & + r_o \frac{\omega_{ie}^2}{\omega_s^2}\underline{U}_4[\frac{1}{2}\omega_s^2 t^2 - (1 - \cos \omega_s t)] + r_o \underline{U}_5 \frac{1}{6}\omega_{ie}^3 t^3\end{aligned} \qquad (3.29)$$

where $\underline{U}_2$ through $\underline{U}_5$ are given by equations (3.29b) through (3.29e).

This equation is plotted in Figure 3.2.

In the following discussion the INS uncertainties are considered less than the values given by Table 3.1.

Accelerometer uncertainties: Bias δf_k Scale factor a_k Bias change ∂f_x, ∂f_y	 < 1 mg < 10^{-4} or 0.01% < 0.1 mg
Gyro uncertainties: Fixed drift rate, ω_{dok} Mass unbalance, ω_{MU_k} (eqn. (3.13a)) $gMUY_k$	 < 10 meru < 5 meru < 10 meru
Alignment uncertainties: Caused by x and y gyro drift Misalignment, ζ_k, $(u)\psi$ Deflection of the vertical, ξ, η	 < 0.1 mrad < 1 mrad or 3.44 min < 0.1 mrad or 20 sec
Initial values: Initial velocity, $\delta V(0)_k$ Latitude error, δL_o Altitude error, δh	 < 0.3 m/s or 1 ft/sec < 0.1 mrad or 20 sec < 100 m

$k = x, y, z \qquad L_o = 45°$

Table 3.1
Constraints on INS Uncertainties

Taking into account only terms giving errors more than 1,300 feet after one and a half hours or terms causing errors above the shaded area in Figure 3.2 when the uncertainties are restricted by the values given in Table 3.1, we can express the coefficient matrices of (3.29), shown in Figure 3.2 as:

$$\underline{\delta V(0)}^{a'} = \begin{bmatrix} \delta V(0)_x \\ \delta V(0)_y \\ \delta V(0)_z \end{bmatrix}$$

Its relative importance decreases with time and can be neglected for t > 60 min. (3.29a)

$$\underline{U}_2 = (\underline{K}_1 - \frac{1}{r_o}\underline{\delta r}(0)^{a'}) = \begin{bmatrix} \partial f_x/g \\ \partial f_y/g \\ \delta f_z/g - a_z - 2\frac{\delta h}{r_o} \end{bmatrix} + \begin{bmatrix} \psi_{\omega y}+\zeta_y \\ -\psi_{\omega x}-\zeta_x \\ 0 \end{bmatrix} \qquad (3.29b)$$

where:

$$\psi_{\omega k(1)} = \omega_{dok}/F(0), \quad \psi_{\omega k(2)} = 0, \quad k = x, y$$

$$\underline{U}_3 = (\underline{K}_2+\underline{K}_3) \approx \begin{bmatrix} \psi_{fz} \cos L_o \\ 0 \\ -\delta f_y/g \cos L_o \end{bmatrix} + \frac{1}{\omega_{ie}} \begin{bmatrix} \omega_{doy}+\omega_{ie}\psi_{\omega z}\cos L_o \\ -\omega_{dox} \\ 0 \end{bmatrix} + \begin{bmatrix} \zeta'_z \cos L_o \\ 0 \\ -\zeta_x \cos L_o \end{bmatrix} \tag{3.29c}$$

where:

$$\psi_{\omega z(1)} \approx 0, \quad \psi_{\omega z(2)} = -\frac{\omega_{doy}}{\omega_{ie} \cos L_o}$$

$$\psi_{fz(1)} = (u)\psi, \quad \psi_{fz(2)} = -\delta f_y/g \tan L_o$$

$$\zeta'_{z(1)} = \zeta_z, \quad \zeta'_{z(2)} = \zeta_z - \zeta_x \tan L_o$$

$$\underline{U}_4 = (\underline{K}_4+2\underline{K}_5) \approx \frac{1}{\omega_{ie}} \begin{bmatrix} 2\omega_{doz} \cos L_o + gMUY_y \\ -\omega_{ie}\psi_{\omega z} \sin L_o \cos L_o - gMUY_x \\ -2\omega_{dox} \cos L_o \end{bmatrix} \tag{3.29d}$$

$$\underline{U}_5 = (-\underline{K}_3+3\underline{K}_6+\underline{K}_7+3\underline{K}_8) \approx \frac{3 \cos L_o}{\omega_{ie}} \begin{bmatrix} -\omega_{doy} \cos L_o - \frac{1}{3}\omega_{ie}\psi_{\omega z} + gMUY_z \\ \omega_{dox} \cos L_o - \omega_{doz} \sin L_o \\ \omega_{doy} \sin L_o - gMUY_x \end{bmatrix} \tag{3.29e}$$

Equation (3.29, a-e) and Figure 3.2 describe the error propagation for INS uncertainties given in Table 3.1 for an uncompensated run lasting less than one and a half hours.

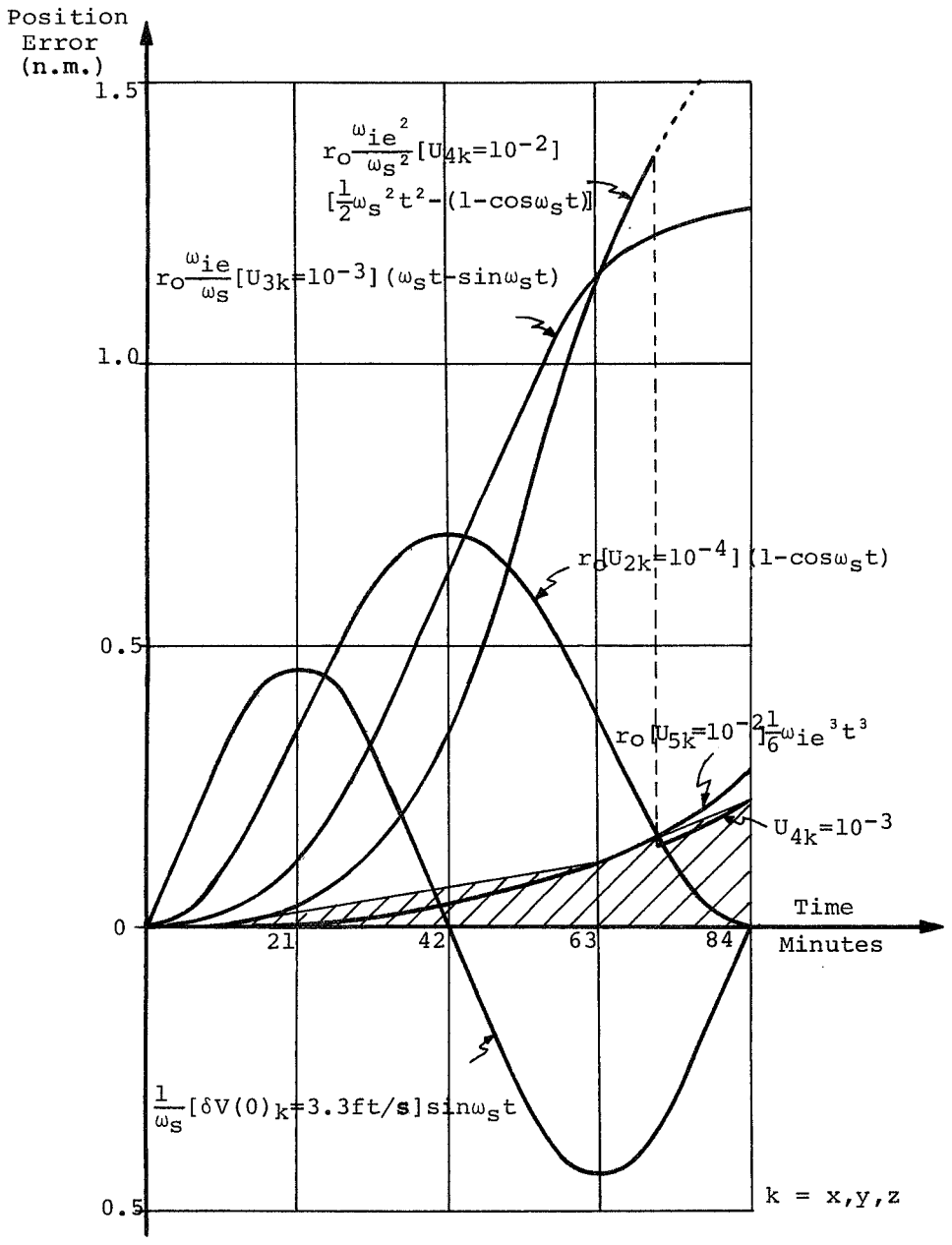

Figure 3.2
Position Error Propagation

As shown, many of the uncertainties giving errors larger than 1 n.m. for a one hour run also give significant errors for times less than 20 minutes, indicating that the most important errors could be detected during a short preflight test run.

In order to visualize how these uncertainty matrices enter into the navigation system, a block diagram valid for a maximum one and a half hour run can be developed. By taking the Laplace transform of equation (3.29), we get:

$$\underline{\delta r}(s)^{a'} = \frac{s\underline{\delta r}(0)^{a'}}{s^2+\omega_s^2} + \frac{\underline{\delta V}(0)^{a'}}{\omega_s}\frac{\omega_s}{s^2+\omega_s^2} + r_o\underline{K}_1\frac{\omega_s^2}{s(s^2+\omega_s^2)}$$

$$+ r_o\frac{\omega_{ie}}{\omega_s}\underline{U}_3\frac{\omega_s^3}{s^2(s^2+\omega_s^2)} \qquad (3.30)$$

$$+ r_o\frac{\omega_{ie}^2}{\omega_s^2}\underline{U}_4\left[\omega_s^2/s^3 - \frac{\omega_s^2}{s(s^2+\omega_s^2)}\right]$$

$$+ r_o\frac{\omega_{ie}^3}{\omega_s^3}\underline{U}_5\left(\frac{\omega_s^3}{s^4} - \frac{\omega_s^3}{s^2(s^2+\omega_s^2)}\right)$$

The last term in the last set of brackets was neglected in equation (3.29). In block diagram form, with all quantities in the a' frame, this becomes:

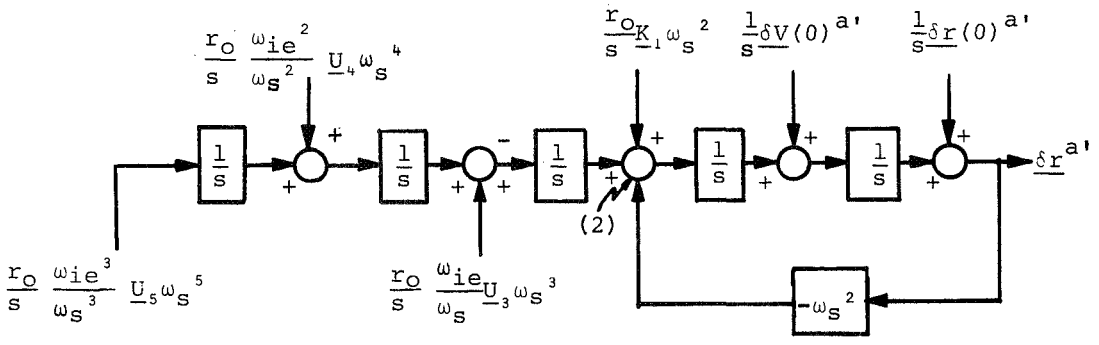

Figure 3.3
Simplified Block Diagram Valid for a Maximum One and a Half Hour Run

By moving the $\frac{1}{s}\underline{\delta r}(0)^{a'}$ term out of the Schuler loop to the output of the system, the $\frac{r_o}{s}\underline{K}_1\omega_s^2$ term will simultaneously be changed to $\frac{r_o}{s}\underline{U}_2\omega_s^2$ which would be more in accordance with the equation (3.29). Note also that $r_o\omega_s^2 = g$. The summation point 2 corresponds to the accelerometer output signals due to INS uncertainties. The other summation points do not correspond to physical summation points in the system.

The following comments can now be made about the interpretation of the $\underline{U}$ matrices.

The $\underline{U}_2$ uncertainty matrix consists of the terms giving rise to actual accelerometer output signals just after the system is switched to the navigation mode. The x and y terms of the $\underline{U}_2$ matrix consists of change in accelerometer bias and misalignment terms causing accelerometer signals. The z term is caused by the erroneous measurement of the g field by the z accelerometer. As can be seen from Figure 3.3, the $\underline{U}_2$ matrix propagates in the same manner as a constant signal from the accelerometer.

The $\underline{U}_3$ matrix is made up of two different error sources propagating in the same manner for short flights. Comparing equation (3.29c) with (2.18a) and remembering that the less important terms have been neglected, we can write:

$$\underline{U}_3 = \begin{bmatrix} C_z' \\ 0 \\ -C_x' \end{bmatrix} \cos L_o + \frac{1}{\omega_{ie}} \begin{bmatrix} \omega_{doy} \\ -\omega_{dox} \\ 0 \end{bmatrix} \tag{3.31}$$

The first term results from the rotation of the g field with respect to the space stabilized platform. After a six hour run, for instance, the g vector has turned 90° and the x accelerometer would pick up an erroneous component of gravity equal to $g\ C_z'\ \cos L_o$. For shorter runs we can make the approximation that the $g\ C_z'\ \cos L_o$ and $-g\ C_x'\ \cos L_o$ terms sensed by the x and z accelerometers grow with $\omega_{ie}t$. The second error source is gyro drift causing an increase in the error angles about the x and y axes. This causes the y and x accelerometers to sense a growing erroneous component of the g field. The $\underline{U}_3$ uncertainty matrix, therefore, propagates similarly to a linearly increasing signal from the accelerometers, as shown in Figure 3.3 where the $\underline{U}_3$ term is fed through an integrator. The advantage of using a gyrocompassing scheme can be seen. The main error contribution to the C_z' error angle is, according to equation (3.29c) and Table 3.1, the term caused by the y gyro drift, $\omega_{ie}\psi_{\omega z(2)}\cos L_o$. This error

causes the x accelerometer to pick up an increasing component of the g vector equal to $\omega_{ie}\psi_{\omega z(2)}$ cos L_o sin $\omega_{ie}t$. The y gyro drift causes a growing misalignment about the y axis equal to $\omega_{doy}t$, making the x accelerometer pick up a component of g equal to g $\omega_{doy}t$. Inserting the expression for $\psi_{\omega z(2)}$ and using $\omega_{ie}t$ instead of sin $\omega_{ie}t$, it can be seen that these two terms are cancelled. Using theodolite alignment of azimuth, the terms (u)ψ cos L_o and ω_{doy}/ω_{ie} will not cancel in general.

The $\underline{U}_4$ matrix also consists mainly of two error sources, namely, constant gyro drift and acceleration-sensitive gyro drift. The increase in the alignment errors about the x and z axes of $\omega_{dox}t$ and $\omega_{doz}t$, respectively, gives an equivalent effect as C_x' and C_z' in equation (3.31). Similarly, the $gMUY_y$ and $gMUY_x$ terms increase the total drift rate of the y and x gyros. These increased gyro drifts cause similar errors as ω_{doy} and ω_{dox} in equation (3.31).

4. PROPAGATION OF I.N.S. UNCERTAINTIES DURING A PREFLIGHT TEST RUN

When alignment to the n frame is finished, the I.N.S. is switched to the navigation mode. A short test run with the vehicle at rest is then performed and the accelerometer and position output data can be analyzed to determine the major error terms. One of the objectives of this analysis is to determine the usefulness of a simple curve-fitting technique.

In a space stabilized system the accelerometer data does not include the Schuler frequency and computer errors. Thus, a comparison between the data received from the accelerometers and from the position computer is made.

4.1 Error Propagation in the Accelerometer Data

The outputs from the accelerometers are given by equation (3.19).

The specific force that the accelerometers should measure can be estimated by:

$$\hat{\underline{f}}^{a'} = \hat{\underline{C}}_n^{a'}\hat{\underline{f}}^n \tag{4.1}$$

where:

$$\hat{\underline{f}}^n = -\hat{\underline{g}}_e^n = -\underline{g}_e^n - \underline{\delta g}_e^n \tag{4.1a}$$

$\underline{\delta g}_e^n$ - uncertainty in estimated magnitude of g

$\hat{\underline{C}}_n^{a'}$ - This estimate is inaccurate because of the uncertainties in the latitude of the vehicle. Using equation (3.20), we get:

$$\hat{\underline{C}}_n^{a'} = \hat{\underline{C}}_i^{a'} \underline{C}_n^i = (\underline{I}+\underline{Z}^a)^{-1} \underline{C}_i^{a'} \underline{C}_n^i \approx (\underline{I}-\underline{Z}^a) \underline{C}_n^{a'} \tag{4.1b}$$

where $\underline{Z}^a$ is given by equation (3.20b)

Putting (4.1a, b) in (3.19) and using the equation $\underline{C}_n^{a'} = \underline{I}+\underline{B}$, we get:

$$\begin{aligned} \underline{\Delta f}^a = \underline{f}_m^a - \hat{\underline{f}}^{a'} = \underline{\delta g}_e^n + \underline{\partial f}^a + (u)\ddot{\underline{r}}^a + \underline{B}(\underline{\delta g}_e^n - \underline{\alpha}^n) - \\ (\underline{\psi}_f^a + \underline{\psi}_\alpha^a)\underline{B}\, \underline{g}_e^n - (\underline{Z}^a + \underline{A}^a + \underline{D}^a + \underline{\psi}_\omega^a + \underline{\psi}_u^a)\underline{C}_n^{a'} \underline{g}_e^n \end{aligned} \tag{4.2}$$

This can be written as a function of time by inserting the expressions for the matrices derived in Chapter 3:

$$\begin{aligned} \underline{\Delta f}^a = g\{&\underline{A}_1 + \underline{K}_2\omega_{ie}t + \underline{A}_3 \sin \omega_{ie}t + \underline{A}_4(1 - \cos \omega_{ie}t) \\ &+ \underline{K}_5\omega_{ie}t \sin \omega_{ie}t + \underline{K}_6\omega_{ie}t\,(1 - \cos \omega_{ie}t) \\ &+ \underline{K}_7(\omega_{ie}t - \sin \omega_{ie}t) + \underline{K}_8 \sin \omega_{ie}t\,(1 - \cos \omega_{ie}t) \\ &+ \underline{K}_9(1 - \cos \omega_{ie}t)^2 + \underline{K}_{10}\sin \omega_{ie}t\,(\omega_{ie}t - \sin \omega_{ie}t) \\ &+ K_{11}(1 - \cos \omega_{ie}t)(\omega_{ie}t - \sin \omega_{ie}t)\} \end{aligned} \tag{4.3}$$

where:

$$\underline{A}_1 = \underline{K}_1 + \frac{1}{g}\begin{bmatrix} (u)\ddot{r}_x \\ (u)\ddot{r}_y \\ (u)\ddot{r}_z + \delta g + 3g\,\dfrac{\delta h}{r_o} \end{bmatrix} \tag{4.3a}$$

$$\underline{A}_3 = \underline{K}_3 + \begin{bmatrix} 0 \\ -(\delta g/g + 3\,\delta h/r_o) \\ 0 \end{bmatrix} \tag{4.3b}$$

$$\underline{A}_4 = \underline{K}_4 + \begin{bmatrix} -(\delta g/g + 3\delta h/r_o)\, \sin L_o \cos L_o \\ 0 \\ -(\delta g/g + 3\delta h/r_o)\, \cos^2 L_o \end{bmatrix} \tag{4.3c}$$

The $\underline{K}_1$ to $\underline{K}_{11}$ matrices are given by the equations (3.25a-k).

The term $(\delta g/g + 3\delta h/r_o)$ is due to a possible difference in computing g in the data analysis and in the navigation computer. It is likely that the same uncertainty is involved. Therefore, for most practical cases this term can be set to zero.

Restricting a preflight test run to a maximum of 20 minutes, equation (4.3) can be simplified considerably. By neglecting terms giving less than 10 μg after 20 minutes for the maximum values of the INS uncertainties given in Table 3.1, and using $\delta g/g = -3\delta h/r_o$, we get:

$$\underline{\Delta f}^a = g\{\underline{A}_1 + \underline{U}_3 \ \omega_{ie} t + \underline{U}_4 \ \frac{1}{2} \omega_{ie}{}^2 t^2\} \tag{4.4}$$

where

$$\underline{A}_1 = \underline{K}_1 + \frac{1}{g}(u)\ddot{\underline{r}}^a \tag{4.4a}$$

$\underline{U}_3$, $\underline{U}_4$ given by equations (3.29c, d)

This result could have been derived directly from Figure 3.3 if the effect of the disturbing accelerations had been added to the accelerometer outputs.

Equation (4.4a) can also be written as:

$$\underline{A}_1 = \underline{U}_2 + \frac{1}{g}(u)\ddot{\underline{r}}^a + \begin{bmatrix} \delta L_o \\ 0 \\ -\delta h/r_o \end{bmatrix} = \underline{U}_2 + \frac{1}{g}(u)\ddot{\underline{r}}^a + \frac{1}{r_o}\underline{\delta r}(0)^a \tag{4.4b}$$

The influence of the uncertainties at different time intervals on the outputs from the accelerometers is given in Table 4.1 as mg or μg per unit of the uncertainty at 45° latitude.

System		Matrix	Units	5 min	10 min	15 min	20 min
1&2	δf_y	$\underline{U}_3$	mg/mg	.015	.031	.049	.061
1&2	δf_z, δg, ∂f_x, ∂f_y	$\underline{A}_1$	mg/mg	1	1	1	1
1&2	a_z	$\underline{A}_1$	µg/PPM	1	1	1	1
1	ω_{dox}, ω_{doy}	$\underline{U}_3$	µg/meru	22	44	66	87
1	ω_{doz}	$\underline{U}_4$	µg/meru	.34	1.3	3.0	5.3
1	$\omega_{dox}/F(0)$, $\omega_{doy}/F(0)$	$\underline{A}_1$	µg/µrad	1	1	1	1
2	ω_{dox}	$\underline{U}_3$	µg/meru	22	44	66	87
2	ω_{doy}, ω_{doz}	$\underline{U}_4$	µg/meru	.34	1.3	3.0	5.3
1&2	$gMUY_x$, $gMUY_y$	$\underline{U}_4$	µg/meru	.24	.95	2.2	3.8
1&2	ζ_x, ζ_y	$\underline{A}_1$	mg/mrad	1	1	1	1
1&2	ζ_z	$\underline{U}_3$	mg/mrad	.015	.031	.049	.061
1	$(u)\psi$	$\underline{U}_3$	mg/mrad	.015	.031	.049	.061

1 mrad ≈ 3.4 $\widehat{\text{min}}$, 1 µrad 0.2 $\widehat{\text{sec}}$, $L_o = 45°$

System 1 - Theodolite alignment of azimuth

System 2 - Gyrocompassing

Table 4.1

The Effect of IMU Uncertainties on Errors in the Accelerometer Outputs

As can be seen from Table 4.1, the main difference between using theodolite alignment of azimuth and gyrocompassing during the alignment mode is the influence of the y gyro drift rate in the navigation mode. From the table it is also obvious that only large drift rates can be detected from the t^2 term in (4.4).

4.2 Propagation of the IMU Uncertainties in the Position Error Data

For preflight test runs lasting less than 20 minutes, equation (3.29) can be simplified further by neglecting terms giving errors *less than 100 feet when the values given in Table 3.1 are used.* Using the position error data from the computer, only the change in the position can be registered. This can be written as:

$$\underline{\Delta r}^{a'} = \underline{\delta r}^{a'} - \underline{\delta r}(0)^{a'}$$

We then get:

$$\underline{\Delta r}^{a'} = \frac{1}{\omega_s}\underline{\delta V}(0)^{a'} \sin \omega_s t + r_o \underline{U}_2 (1 - \cos \omega_s t) + r_o \frac{\omega_{ie}}{\omega_s} \underline{U}_3 (\omega_s t - \sin \omega_s t) + r_o \frac{\omega_{ie}^2}{\omega_s^2} \underline{U}_4 [\frac{1}{2} \omega_s^2 t^2 - (1 - \cos \omega_s t)] \quad (4.5)$$

where the matrices are given by (3.29a-d).

Only drift rates larger than 4-6 meru will give a position error larger than 100 feet in the last term of (4.5). Therefore, it is rather doubtful whether this term can be detected in a preflight test run.

The effects of the most important I.N.S. uncertainties involved in equation (4.5) are listed in Table 4.2 for $L_o = 45°$.

System	Uncertainty	Matrix	Units	5 min	10.5 min	15 min	20 min
1&2	δf_y	$\underline{U}_3$	ft/mg	8	78	190	492
1&2	δf_z, ∂f_x, ∂f_y	$\underline{U}_2$	ft/mg	1440	6130	11840	21000
1&2	a_z	$\underline{U}_2$	ft/PPM	1.4	61	11.8	21
1&2	ω_{dox}	$\underline{U}_3$	ft/meru	11.5	95	269	700
1	ω_{doy}	$\underline{U}_3$	ft/meru	11.5	95	269	700
1&2	ω_{doz}	$\underline{U}_4$	ft/meru	.1	1.4	6	23
1	$\omega_{dox}/F(0)$, $\omega_{doy}/F(0)$	$\underline{U}_2$	ft/μrad	1.3	6.1	11.8	21
1&2	$gMUY_x$, $gMUY_y$	$\underline{U}_4$	ft/meru	.06	1	4.6	16.4
1&2	ζ_x, ζ_y	$\underline{U}_2$	ft/mrad	1440	6130	11840	21000
1&2	ζ_z	$\underline{U}_3$	ft/mrad	8	78	190	492
1	$(u)\psi$	$\underline{U}_3$	ft/mrad	8	78	190	492
1&2	$\delta V(0)_k$, k = x, y, z		ft/ft/s	292	565	720	800
1&2	δh	$\underline{U}_2$	ft/ft	.002	.03	.13	.46

$L_o = 45°$, 1 μrad ≈ .2 sec, 1 mrad ≈ 3.4 min

System 1 - Theodolite alignment of azimuth

System 2 - Gyrocompassing

Table 4.2

The Effect of I.N.S. Uncertainties on the Position Error during a Preflight Test Run

4.3 Estimation of I.N.S. Uncertainties from a Preflight Test Run

By comparing equation (4.4) for the accelerometer output error with equation (4.5) for the position error, we find that essentially the same uncertainty matrices are involved. For test times less than 15 minutes, we get:

$$\sin \omega_s t \approx \omega_s t,$$

$$1 - \cos \omega_s t \approx \frac{1}{2} \omega_s{}^2 t^2,$$

$$\omega_s t - \sin \omega_s t \approx \frac{1}{6} \omega_s{}^3 t^3,$$

and

$$\frac{1}{2} \omega_s{}^2 t^2 - (1 - \cos \omega_s t) \approx \frac{1}{24} \omega_s{}^4 t^4$$

The position errors are then approximately the double integral of the accelerometer output errors because the error contributions from the navigation computer is negligible or cause the same uncertainties as the uncertainties in the estimation of the specific force used to compute the accelerometer output errors except for the $\underline{\delta r}(0)^a$ term, equation (4.4b). The $(u)\underline{\ddot{r}}^a$ term will be filtered out in the integration. The "open loop double integration" effect arises because the test time, which is less than one fourth of a Schuler period, prevents us from getting any benefit from the Schuler tuning in bounding the errors.

The uncertainty in the initial velocity setting can give a negligible position error if the accelerometer signals are properly filtered. The maximum value of the velocity uncertainty corresponds to the amplitude of the output from the first integrator in the navigation computer caused by the wiggling of the vehicle on the ground. The $\underline{\delta V}(0)^{a'}$ term is constant during the navigation mode and is caused by switching the system from the alignment mode to the navigation mode when the instantaneous velocity is different from zero (Only the mean value of the ground speed, in this case zero, is fed to the navigation computer). If this velocity uncertainty is of importance, it can be computed during the alignment phase. The $\underline{\delta V}(0)^{a'}$ term propagates with $\sin \omega_s t$ and can easily be detected during the test run. This uncertainty will, of course, differ from alignment to alignment.

The $(u)\underline{\ddot{r}}$ term detected by the accelerometers is also caused by the same wiggling of the vehicle. This disturbance will make the accelerometer data noisy so that a low pass filtering of the accelerometer data is necessary. It therefore seems simpler to use the position data

for estimating the I.N.S. uncertainties because of the filtering effect of the double integration.

When using pulse restraint accelerometers, each pulse corresponds to a fixed velocity increment, ΔV. This gives a finite resolution during a limited test interval.

If the number of the velocity increments due to the IMU uncertainties during the test interval T is N for the three accelerometer outputs, we can write:

$$\int_0^T \underline{\underline{\Delta f}}^a \, dt = \underline{N} \, \Delta V$$

which gives:

$$\underline{A}_1 + \underline{U}_3 \frac{1}{2} \omega_{ie} T + \underline{U}_4 \frac{1}{6} \omega_{ie}{}^2 T^2 = \frac{N \Delta V}{\underline{\underline{T}} g}$$

In order to be able to determine the coefficients for the three time functions of equation (4.4), a minimum requirement is:

$$N \geq 3$$

Requiring that each of the coefficients shall give at least three pulses during the test period, we get the following minimum values that the coefficient must have in order to be determined:

$$A_{1k} \geq \frac{3\Delta V}{Tg} \qquad \underline{U}_{3k} \geq \frac{6\Delta V}{\omega_{ie} T^2 g}$$

$$\underline{U}_{4k} \geq \frac{18\Delta V}{\omega_{ie}{}^2 T^3 g} \qquad k = x, y, z \tag{4.6}$$

For $\Delta V = 0.1$ ft/sec, we get the following minimum values for different durations of the test run:

Coef. \ T	5 min	10 min	15 min	20 min
A_{1k}	31×10^{-6}	15.5×10^{-6}	10.4×10^{-6}	7.76×10^{-6}
U_{3k}	2.84×10^{-3}	0.71×10^{-3}	0.32×10^{-3}	0.18×10^{-3}
U_{4k}	0.39	49×10^{-3}	14.5×10^{-3}	6.1×10^{-3}

Table 4.3

Minimum Values of the Coefficients which can be Detected for $\Delta V = 0.1$ ft/sec

The matrix $\underline{U}_4$ in equation (4.4) consists of gyro drift terms. These drift terms must exceed the following values in order to be detected ($L_o = 45°$):

	10 min	15 min	20 min
$gMUY_x$, $gMUY_y$ meru	49	14.5	6.1
ω_{doz} meru	35	10	4.3

i.e., only large drift rates will show up.

Restricting the discussion of the maximum values given by Table 3.1, it is not likely that the $\underline{U}_4$ matrix can be determined for test times less than 15 minutes or even 20 minutes because in addition to the bad resolution, we can also have estimation errors.

The U_{3k} coefficients (k = x, y using theodolite alignment of azimuth, k = y when using gyrocompassing), has a resolution for T = 10 minutes better than 1 meru. If a minimum of 10 pulses from the accelerometers are required, a 15 minute test run is necessary. To determine the U_{3z} term at least 15 minutes of testing time is necessary.

The resolution of the A_{1k} terms are 15.5 μrad, corresponding to 15.5 μg for T = 10 minutes.

This leads to the conclusion that only the $\underline{A}_1$ and the $\underline{U}_3$ matrices in equation (4.4) can be determined. Provided that the resolution of the computed position does not give further limitations (resolution better than a few feet is required), the result above is also valid for the position error; i.e. if the t^2 term in the accelerometer output error equation cannot be determined, its double integrated value, or more precisely, the $\underline{U}_4$ matrix in equation (4.5) cannot be determined either. Substituting $\underline{U}_2$ for $\underline{A}_1$, Table 4.3 is also valid for the position error equation.

Equation (4.5) can then be written as:

$$\underline{\Delta r}^{a'} = \frac{1}{\omega_s} \underline{\delta V}(0)^{a'} \sin \omega_s t + r_o \underline{U}_2 (1 - \cos \omega_s t) + r_o \frac{\omega_{ie}}{\omega_s} \underline{U}_3 (\omega_s t - \sin \omega_s t) \qquad (4.7)$$

The coefficients in the above equation can be estimated from the preflight test data:

$$\hat{\underline{U}}_1 = \underline{\delta V}(0)^{a'} + \underline{E}_1 \qquad (4.8a)$$

$$\hat{\underline{U}}_2 = \underline{U}_2 + \underline{E}_2 \qquad (4.8b)$$

$$\hat{\underline{U}}_3 = \underline{U}_3 + \underline{E}_3 \qquad (4.8c)$$

where

$$\underline{E}_i = \{\varepsilon_{ix}, \varepsilon_{iy}, \varepsilon_{iz}\} \qquad i = 1, 2, 3$$

are the errors in the estimates and

$\underline{\delta V}(0)^{a'}$, $\underline{U}_2$ and $\underline{U}_3$ are given by the equations (3.29a, b, c)

Equations (4.8b, c) can now be written as:

$$\hat{\underline{U}}_2 = \begin{bmatrix} \partial f_x/g + \zeta_y + \varepsilon_{2x} \\ \partial f_y/g - \zeta_x + \varepsilon_{2y} \\ (\delta f_z/g - a_z - 2\delta h/r_o) + \varepsilon_{2z} \end{bmatrix} + \begin{bmatrix} \omega_{doy}/F(0) \\ -\omega_{dox}/F(0) \\ 0 \end{bmatrix}_{(1)} \tag{4.9a}$$

$$\hat{\underline{U}}_3 = \begin{bmatrix} \zeta_z \cos L_o + \varepsilon_{3x} \\ -\omega_{dox}/\omega_{ie} + \varepsilon_{3y} \\ -(\delta f_y/g + \zeta_x)\cos L_o + \varepsilon_{3z} \end{bmatrix} + \begin{bmatrix} \omega_{doy}/\omega_{ie} + (u)\psi\cos L_o \\ 0 \\ 0 \end{bmatrix}_{(1)}$$

$$+ \begin{bmatrix} -(\delta f_y/g + \zeta_x)\sin L_o \\ 0 \\ 0 \end{bmatrix}_{(2)} \tag{4.9b}$$

For the interpretation of these two matrices, see the end of Chapter 3.

It is evident from these equations that we get no information about the x accelerometer bias and the z gyro drift(and y gyro drift for system 2).

The $(\delta f_z/g - a_z - 2\delta h/r_o)$ term, which is dominated by the constant bias term, can be regarded as one unknown. The reason is that this term can be thought of as an erroneous measurement of the g vector, and the a_z and δh terms are neglected in the other uncertainty matrices.

For system 1 equations (4.9a, b) can be said to contain 10 unknown and independent I.N.S. uncertainties, plus six estimation error terms, while we have only six known (estimated) terms. The I.N.S. terms for system 1 are

$$(u)\underline{x}_{INS(1)} = \{\partial f_x, \partial f_y, (\delta f_z/g - a_z - 2\delta h/r_o), \delta f_y, \zeta_x, \zeta_y, \zeta_z, (u)\psi, \omega_{dox}, \omega_{doy}\} \tag{4.10a}$$

Using system 2 equations (4.9a, b) contain eight independent I.N.S. uncertainties.

$$(u)\underline{x}_{INS(2)} = \{\partial f_x,\ \partial f_y,\ (\delta f_z/g - a_z - 2\delta h/r_o),\ \delta f_y,\ \zeta_x,\ \zeta_y,\ \zeta_z,\ \omega_{dox}\} \tag{4.10b}$$

It is not obvious that any of these terms can be neglected in order to reduce these two uncertainty vectors.

It should also be noted that the estimation errors in equations (4.9a, b) could be at least of the same order of magnitude as the figures given in Table 4.3, rows 1 and 2, respectively.

As a conclusion it can be stated that it is not possible from a preflight test run only to determine the independent I.N.S. uncertainties separately.

5. COMPENSATION OF I.N.S. UNCERTAINTIES

How to use the estimated data found from the preflight test run to compensate for the I.N.S. uncertainties depends upon the updating procedure chosen. The different approaches described here are:

1. The coefficients for the different time functions are interpreted as misalignment, bias and drift rates. After compensation a realignment is performed.

2. Using only the position error data, compensation signals are applied without realignment.

3. Using accelerometer data to derive compensation signals which are applied without realignment.

4. The uncertainties are determined using only data from the alignment phase.

Methods 2 and 3 imply that the compensation data can be applied immediately after the test run is finished.

Figure 5.1 shows some possible points where compensation signals can be fed into the system.

5.1 Compensation of the Uncertainties Followed by a Realignment

If the main I.N.S. uncertainties remain almost constant from alignment to alignment, which should be a valid assumption when the time involved is less than a half hour and there is no cooling down or spin motor rundown between the alignments, one could determine the

uncertainties from a preflight test run, derive compensation signals and then realign the system.

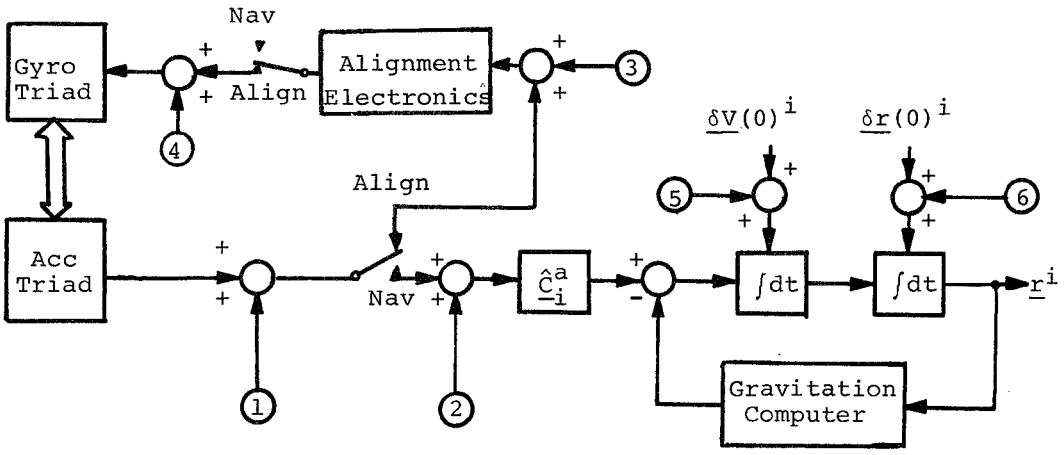

Figure 5.1
Principal Block Diagram Showing Alignment and Navigation Mode

The constant terms in $\underline{\delta V}(0)^{a'}$ are negligible. The random terms caused by the motion of the vehicle will vary from alignment to alignment, and no compensation signal should be applied.

Ideally, only the constant parts of the uncertainty terms should be compensated for, but we cannot distinguish between constant and random terms from the test run only, other than by using the knowledge we have of the nature of the uncertainty sources.

Going back to equations (4.8a) and (4.9a, b), we can split those equations up into constant terms and terms varying from alignment to alignment. Using no subscript or subscript c for constant terms, r for random, and letting $(\ )_p$ denote the value during the preflight test run, we can write:

$$\hat{\underline{U}}_1 = \underline{\delta V}(0)^{a'}_r + \underline{E}_1 \qquad (5.1a)$$

The constant terms in $\underline{\delta V}(0)^{a'}$ are negligible. The random terms caused by the motion of the vehicle will vary from alignment to alignment, and no compensation signal should be applied.

$$\hat{\underline{U}}_2 = \begin{bmatrix} \partial f_{cx}/g + \zeta_{cy} + (\partial f_{rx}/g + \zeta_{ry})_p + \varepsilon_{2x} \\ \partial f_{cy}/g - \zeta_{cx} + (\partial f_{ry}/g - \zeta_{rx})_p + \varepsilon_{2y} \\ \delta f_z/g - a_z - 2\delta h/r_o + \varepsilon_{2z} \end{bmatrix} + \begin{bmatrix} (\omega_{doy}/F(0)_p \\ (-\omega_{dox}/F(0)_p \\ 0 \end{bmatrix}_{(1)} \tag{5.1b}$$

$$\hat{\underline{U}}_3 = \begin{bmatrix} \zeta_{cz} \cos L_o + (\zeta_{rz} \cos L_o)_p + \varepsilon_{3x} \\ -\omega_{dox}/\omega_{ie} + \varepsilon_{3y} \\ -(\delta f_y/g + \zeta_{cx}) \cos L_o - (\zeta_{rx} \cos L_o)_p + \varepsilon_{3z} \end{bmatrix}$$

$$+ \begin{bmatrix} \omega_{doy}/\omega_{ie} + (u)\psi \cos L_o \\ 0 \\ 0 \end{bmatrix}_{(1)} + \begin{bmatrix} -(\delta f_y/g + \zeta_{cx}) \sin L_o - (\zeta_{rx} \sin L_o)_p \\ 0 \\ 0 \end{bmatrix}_{(2)} \tag{5.1c}$$

The terms ζ_{rk}, k = x, y, z can be thought of as misalignments varying from alignment to alignment due to transients or limit cycles as described in Chapter 2, succeeding equation (2.17d), while ζ_{ck} can be thought of as constant electrical offsets in the alignment electronics, equations (2.11a) and (2.15a). The ζ_{ck} terms should therefore ideally be compensated for at point 3, Figure 5.1.

The bias changes ∂f_k, k = x, y, defined in conjunction with equations (3.18), probably contain mainly constant terms and should be compensated for at point 2, Figure 5.1.

The gyro drift terms should be compensated for at point 4, Figure 5.1.

As explained in the last paragraph of Chapter 4, we do not have enough information to compute the various terms of equations (5.1b, c). The simplest and probably the best way of using the $\hat{\underline{U}}_2$ matrix is to derive the following compensation signals which should be summed into point 2, Figure 5.1:

$$\underline{f}^a_{cp} \approx \begin{bmatrix} f_{cpx} \\ f_{cpy} \\ f_{cpz} \end{bmatrix} = -g\, \hat{\underline{U}}_2 \tag{5.2}$$

where the signal, f_{cpk}, k = x, y, z, should be added to the k^{th} accelerometer signal.

This will be the best way to compensate for the bias changes,

equation (5.1b) or (4.9a, b). The accelerometer signals due to the misalignment terms in the $\underline{U}_2$ matrix will also be compensated correctly for short runs, while, when the length of the run approaches six hours (90° rotation of the g vector), this compensation becomes less and less accurate. Applying only $\underline{f}^a_{cp}$ as a compensation signal and realigning the platform, the alignment errors have not been reduced, but the effect of the misalignment on the position error has been reduced.

The error propagation after compensation and realignment will depend upon how the $\underline{U}_{3k}$ terms are applied. Here we shall distinguish between methods which differ by where the compensation signals are applied.

5.1.1 Interpreting the U_{3k} Terms as Linearly Increasing Accelerometer Uncertainties

This interpretation follows directly from Figure 3.3 where the $\underline{U}_3$ matrix is integrated and added to point 2, which corresponds to the errors in the accelerometer signals. The effect of the $\underline{U}_3$ uncertainty matrix could then be counteracted by applying $g\omega_{ie}\hat{\underline{U}}_{3k}$, k = x, y, z to integrators whose outputs are connected to point 2, Figure 5.1. The input to the three integrators will then be:

$$p\underline{f}'_{cp} = \begin{bmatrix} pf'_{cpx} \\ pf'_{cpy} \\ pf'_{cpz} \end{bmatrix} = -g\omega_{ie}\hat{\underline{U}}_3 \tag{5.3}$$

Using $\underline{f}^a_{cp}$, equation (5.2), as compensation signals at point 2, and $p\underline{f}'^a_{cp}$, equation (5.3), through integrators to point 2 followed by a realignment of the platform, the resulting error propagation valid for a maximum one and a half hour run can be found from Figure 3.3 or equation (3.30). Transformed to the time domain, this equation becomes:

$$\begin{aligned} \underline{\delta r}(t)^{a'} = {} & \underline{\delta r}(0)^{a'} + \frac{1}{\omega_s}\underline{\delta V}(0)^{a'}\sin\omega_s t \\ & + r_o(\underline{U}_2 - \hat{\underline{U}}_2)(1 - \cos\omega_s t) \\ & + r_o\frac{\omega_{ie}}{\omega_s}(\underline{U}_3 - \hat{\underline{U}}_3)(\omega_s t - \sin\omega_s t) \\ & + r_o\frac{\omega_{ie}^2}{\omega_s^2}\underline{U}_4\left[\tfrac{1}{2}\omega_s^2 t^2 - (1 - \cos\omega_s t)\right] + r_o\underline{U}_5\tfrac{1}{6}\omega_{ie}^3 t^3 \end{aligned} \tag{5.4}$$

where the following relation was used:

$$\underline{\delta r}(0)^{a'} \cos \omega_s t + r_o \underline{K}_1 (1 - \cos \omega_s t) = \underline{\delta r}(0)^{a'} + r_o \underline{U}_2 (1 - \cos \omega_s t)$$

This then becomes:

Propagated with r_o $(1 - \cos \omega_s t)$:

$$\underline{U}_2^1 = \begin{bmatrix} (\partial f_{rx}/g + \zeta_{ry} - (\partial f_{rx}/g + \zeta_{ry})_p - \varepsilon_{2x} \\ (\partial f_{ry}/g - \zeta_{rx})_n - (\partial f_{ry}/g - \zeta_{rx})_p - \varepsilon_{2y} \\ -\varepsilon_{2z} \end{bmatrix} \tag{5.4a}$$

where

$$(\omega_{dok}/F(0)) = (\omega_{dok}/F(0))_p \text{ (Gyro drift not compensated for)}$$

Propagated with $r_o \frac{\omega_{ie}}{\omega_s} (\omega_s t - \sin \omega_s t)$:

$$\underline{U}_3^1 = \begin{bmatrix} [(\zeta_{rz})_n - (\zeta_{rz})_p] \cos L_o - \varepsilon_{3x} \\ -\varepsilon_{3y} \\ [-(\zeta_{rx})_n + (\zeta_{rx})_p] \cos L_o - \varepsilon_{3z} \end{bmatrix} + \begin{bmatrix} -[(\zeta_{rx})_n - (\zeta_{xx})_p] \sin L_o \\ 0 \\ 0 \end{bmatrix}_{(2)} \tag{5.4b}$$

where terms less than 10^{-4} have been neglected.

The last two terms remain the same as in equation (3.29d, e). The conclusion that can be drawn is that only the $(1 - \cos \omega_s t)$ and the $(\omega_s t - \sin \omega_s t)$ terms have been reduced by this compensation method while the other terms remain unchanged. From Figure 3.2 it is evident that the $\underline{U}_4$ term, which contains acceleration-sensitive drift rates for the x and y gyros, together with the initial z gyro drift, can give a significant position error. Table 5.1 shows the effect of the residual drift terms for L = 45°.

Items	Matrix	Units	Position Error		
			42 Min	63 Min	84 Min
$\delta V(0)_k$, k=x,y,z	$\underline{\delta V}(0)$[a]	ft/ft	0	800	0
$\underline{U}'_{2k}$, k=x,y,z	$\underline{U}'_2$	ft/10^{-4}	4200	2100	0
$\underline{U}'_{3k}$, k=x,y,z	$\underline{U}'_3$	ft/10^{-3}	3840	6980	7670
ω_{dok}, k=x,z	$\underline{U}'_4$	ft/meru	297	974	1940
$gMUY_k$, k=x,y		ft/meru	210	688	1405
$\omega_{doy(2)}$		ft/meru	148	488	984
ω_{doz}	$\underline{U}'_5$	ft/meru	33	100	256
$gMUY_z$		ft/meru	46	151	360

Table 5.1
Effect of Uncompensated Uncertainties after Realignment

The major disadvantages with this method of using the information in the $\hat{U}_3$ matrix are:

a) Three extra integrators in the compensation electronics are required.

b) The magnitude of the $\underline{U}_4$ and $\underline{U}_5$ matrices has not been reduced.

The advantage is that the effect of the $\underline{U}_3$ matrix has been reduced as much as possible leaving only unpredictable terms. As can be seen from Figure 3.2, the sensitivity of the U_{3k} terms, k = x, y, z, on the position error are approximately ten times the sensitivity of the U_{4k} terms.

5.1.2 Supplying Compensation Signals Derived from the $\hat{U}_3$ Matrix to the Gyro Torquers

With a compensation and a subsequent realignment, it is evident from the expressions for the $\underline{U}$ matrices in equation (3.29) that only the terms containing ω_{dok}, k = x, y, z can be controlled by applying compensation signals to the gyro torquers. Because the $\hat{\underline{U}}_2$ and $\hat{\underline{U}}_3$ matrices, equation (5.1b, c), do not give us any information about ω_{doz} or (ω_{doy} for system 2), we cannot gain anything by applying torquer signals to the z, respective z and y gyros.

The compensation signals to be applied at point 4, Figure 5.1 can, by using (5.1c), be expressed as:

$$\underline{\omega}^{a}_{cp(1)} = \omega_{ie}\begin{bmatrix}\hat{U}_{3y}\\ -\hat{U}_{3x}\\ 0\end{bmatrix} = \begin{bmatrix}-\omega_{dox} + \omega_{ie}\varepsilon_{3y}\\ -\omega_{doy}-\omega_{ie}(\zeta_{cz}+(u)\psi)\cos L_o-\omega_{ie}(\zeta_{rz}\cos L_o)_p-\omega_{ie}\varepsilon_{3x}\\ 0\end{bmatrix} \tag{5.5a}$$

and for system 2:

$$\underline{\omega}^{a}_{cp(2)} = \omega_{ie}\begin{bmatrix}\hat{U}_{3y}\\ 0\\ 0\end{bmatrix} = \begin{bmatrix}-\omega_{dox} + \omega_{ie}\varepsilon_{3y}\\ 0\\ 0\end{bmatrix} \tag{5.5b}$$

The residual gyro drifts after compensation are:

$$\underline{\omega}'^{a}_{do} = \underline{\omega}^{a}_{do} + \underline{\omega}^{a}_{cp} = \begin{bmatrix}\omega_{dox}\\ \omega_{doy}\\ \omega_{doz}\end{bmatrix} + \omega_{ie}\begin{bmatrix}\hat{U}_{3y}\\ 0\\ 0\end{bmatrix} + \omega_{ie}\begin{bmatrix}0\\ -\hat{U}_{3x}\\ 0\end{bmatrix}_{(1)}$$

or:

$$\underline{\omega}'^{a}_{do(1)} = \omega_{ie}\begin{bmatrix}\varepsilon_{3y}\\ -(\zeta_{cz}+(u)\psi)\cos L_o - (\zeta_{rz}\cos L_o)_p - \varepsilon_{3x}\\ \omega_{doz}/\omega_{ie}\end{bmatrix} \tag{5.6a}$$

$$\underline{\omega}'^{a}_{do(2)} = \begin{bmatrix}\omega_{ie}\varepsilon_{3y}\\ \omega_{doy}\\ \omega_{doz}\end{bmatrix} \tag{5.6b}$$

Inserting equation (5.2) as a compensation signal at point 2, and equation (5.5a) or (5.5b) at point 4, Figure 5.1, and realigning the platform, the equation in the time domain can be derived in a similar way as equation (5.4):

$$\underline{\delta r}(t)^{a'} = \underline{\delta r}(0)^{a'} + \frac{1}{\omega_s}\underline{\delta V}(0)^{a'}\sin\omega_s t + r_o(\underline{U}'_2-\hat{\underline{U}}_2)(1-\cos\omega_s t)$$

$$+ r_o\frac{\omega_{ie}}{\omega_s}\underline{U}'_3\ (\omega_s t - \sin\omega_s t) +$$

$$+ r_o \frac{\omega_{ie}^2}{\omega_s^2} \underline{U}_4' \left[\frac{1}{2}\omega_s^2 t^2 - (1 - \cos \omega_s t)\right] + r_o \underline{U}_5' \frac{1}{6}\omega_{ie}^3 t^3 \quad (5.7)$$

where the prime on the $\underline{U}$ matrices indicate that $\underline{\omega}_{do}'$ has been substituted for ω_{do}.

Using the same notation as was explained in paragraph 5.1.1, we get:

$$\underline{U}_2' - \hat{\underline{U}}_2 = \begin{bmatrix} (\partial f_{rx}/g+\zeta_{ry})_n - (\partial f_{rx}/g+\zeta_{ry})_p - \varepsilon_{2x} \\ (\partial f_{ry}/g-\zeta_{rx})_n - (\partial f_{ry}/g-\zeta_{rx})_p - \varepsilon_{2y} \\ -\varepsilon_{2z} \end{bmatrix} + \begin{bmatrix} -(\omega_{doy}/F(0)_p \\ (\omega_{dox}/F(0)_p \\ 0 \end{bmatrix}_{(1)} \quad (5.7a)$$

where $(\omega_{dok}/F(0))_n \approx 0$ due to the gyro drift compensation.

$$\underline{U}_3' = \begin{bmatrix} 0 \\ -\varepsilon_{3y} \\ -(\delta f_y/g+\zeta_x)\cos L_o \end{bmatrix} + \begin{bmatrix} [(\zeta_{rz})_n - (\zeta_{rz})_p]\cos L_o - \varepsilon_{3x} \\ 0 \\ 0 \end{bmatrix}_{(1)}$$

$$+ \begin{bmatrix} [\zeta_z - (\delta f_y/g+\zeta_x)\tan L_o]\cos L_o \\ 0 \\ 0 \end{bmatrix}_{(2)} \quad (5.7b)$$

$$\underline{U}_4' = \frac{1}{\omega_{ie}} \begin{bmatrix} 2\omega_{doz}\cos L_o + gMUY_y \\ -gMUY_x \\ -2\,\omega_{ie}\,\varepsilon_{3y}\cos L_o \end{bmatrix} + \omega_{doy} \begin{bmatrix} 0 \\ \sin L_o \\ 0 \end{bmatrix}_{(2)} \quad (5.7c)$$

$$\underline{U}_5' = \frac{3\cos L_o}{\omega_{ie}} \begin{bmatrix} gMUY_z \\ -\omega_{doz}\sin L_o \\ -gMUY_x \end{bmatrix} + \frac{1}{\omega_{ie}} \begin{bmatrix} -\omega_{doy}(3\cos^2 L_o - 1) \\ 0 \\ 3\omega_{doy}\sin L_o \cos L_o \end{bmatrix}_{(2)} \quad (5.7d)$$

where terms less than 10^{-3} have been neglected.

Comparing this result with the result obtained in paragraph 5.1.1, we see that the following terms have increased in magnitude:

$U'_{2x(1)}$, $U'_{2y(1)}$, $U'_{3x(2)}$, U'_{3z},

while the terms which have been reduced are:

U'_{4z}, $\underline{U}'_{5(1)}$, $U'_{5y(2)}$

The effect of these changes can be found from Figure 3.2.

The reason that this method gives a less favorable result for the $\underline{U}'_3$ matrix than the method described in paragraph 5.1.1, is that some of the information in the $\underline{\hat{U}}_3$ matrix is not used. A very useful solution would be to combine these two methods by applying $\hat{U}_{3z}$, respectively $\hat{U}_{3x}$ and $\hat{U}_{3z}$ for system 2 through integrators to point 2, Figure 5.1. When judging other methods, one should avoid $\underline{E}_3$ error terms in the compensated $\underline{U}'_2$ matrix because these error terms could be larger than the original uncertainty terms in the $\underline{U}_2$ matrix.

These compensation schemes will be of limited value when the random misalignment terms dominate and when the initial velocity error cannot be neglected. Another disadvantage of these schemes is that the realignment is time consuming (5-15 minutes could be practical figures), making the preflight preparations in many cases unacceptably long.

5.2 Compensation Using Position Error Data without a Following Realignment

Instead of realigning the platform after a compensation of the uncertainties has been performed, we can apply the compensation terms when the preflight test run is finished and reset the position and velocity integrators to the correct values. It is assumed that the estimated values of the uncertainties are available and put into the I.N.S. computer just after the preflight test run is finished. Referring to Figure 5.1, position error is compensated for at 6, velocity error at 5, initial misalignment error and misalignment error caused by constant gyro drift (acceleration-sensitive drift rates cannot be estimated from a short test run) at point 2, and the linearly increasing acceleration signals via integrators to point 2, i.e. the same method of using the $\underline{\hat{U}}_2$ matrix as in paragraph 5.1.1, has been used for convenience. In addition to the information needed for the schemes described in paragraph 5.1, here we also need the correct value of the velocity and position in the i-frame at the time T when the test run is finished.

The following signals are then inserted as step functions at t = T. Expressed in Laplace form and referring to Figure 3.3, we have:

at point 6: $-\frac{1}{s}\,\underline{\delta\hat{r}}(T)^{a'}\varepsilon^{-sT}$

where $\underline{\delta\hat{r}}(T)^{a'}$ is the estimated position error at t = T

at point 5: $-\frac{1}{s}\,\underline{\delta\hat{\dot{r}}}(T)^{a'}\varepsilon^{-sT}$

where $\underline{\delta\hat{\dot{r}}}(T)^{a'}$ is the estimated velocity error at t = T

at point 2: $-r_o\frac{\omega_s^2}{s}\,(\hat{\underline{U}}_2 + \frac{\omega_{ie}}{\omega_s}\,\hat{\underline{U}}_3\,\omega_s T)\,\varepsilon^{-sT}$

at integrators to point 2: $-\frac{\omega_s^3}{s}\,r_o\,\frac{\omega_{ie}}{\omega_s}\,\hat{\underline{U}}_3\,\varepsilon^{-sT}$

In the time domain we then get:

$$\underline{\delta r}(t)^{a'} - \underline{\delta r}(0)^{a'} = -\underline{\delta\hat{r}}(T)^{a'}\cos\omega_s(t-T) + \frac{1}{\omega_s}\,\underline{\delta V}(0)^{a'}\sin\omega_s t$$

$$-\frac{1}{\omega_s}\,\underline{\delta\hat{\dot{r}}}(T)\sin\omega_s(t-T) + r_o\,\underline{U}_2(1-\cos\omega_s t)$$

$$- r_o\,(\hat{\underline{U}}_2 + \hat{\underline{U}}_3\,\omega_{ie}T)(1-\cos\omega_s(t-T)) + r_o\,\frac{\omega_{ie}}{\omega_s}\,\underline{U}_3$$

$$(\omega_s t - \sin\omega_s t) - r_o\,\frac{\omega_{ie}}{\omega_s}\,\hat{\underline{U}}_3[\omega_s(t-T) - \sin\omega_s(t-T]$$

$$+ r_o\,\frac{\omega_{ie}^2}{\omega_s^2}\,\underline{U}_4\,[\tfrac{1}{2}\,\omega_s^2 t^2 - (1-\cos\omega_s t)] + r_o\,\underline{U}_5\tfrac{1}{6}\,\omega_{ie}^3 t^3 \qquad (5.8)$$

From equation (3.29) we find:

$$\underline{\delta r}(T)^{a'} - \underline{\delta r}(0)^{a'} = + \frac{1}{\omega_s}\,\underline{\delta V}(0)^{a'}\sin\omega_s T$$

$$+ r_o\,\underline{U}_2\,(1-\cos\omega_s T) + r_o\frac{\omega_{ie}}{\omega_s}\,\underline{U}_3(\omega_s T - \sin\omega_s T)$$

$$+ r_o\,\frac{\omega_{ie}^2}{\omega_s^2}\,\underline{U}_4\,[\tfrac{1}{2}\,\omega_s^2 T^2 - (1-\cos\omega_s T)] + r_o\underline{U}_5\tfrac{1}{6}\,\omega_{ie}^3 T^3 \qquad (5.8a)$$

Resetting the position integrator to the calculated correct value corresponds to putting in a step equal to:

$$\underline{\delta\hat{r}}(T)^{a'} = \underline{\delta r}(T)^{a'} - \underline{\delta r}(0)^{a'} - \underline{\varepsilon r}(T)^{a'} \qquad (5.8b)$$

The correct position is not known exactly because of the position uncertainty of the vehicle. The term $\underline{\varepsilon r}(T)^{a'}$ accounts for inaccuracies in calculating what the position should be at t = T.

The velocity at t = T is:

$$\frac{d}{dt}\,\underline{\delta r}(t)^{a'}\Big|_{t=T} = \underline{\delta \dot{r}}(T)^{a'} = +\,\omega_s\,[\frac{1}{\omega_s}\,\underline{\delta V}(0)^{a'}\cos\omega_s T$$

$$+\,r_o\,\underline{U}_2\sin\omega_s T + r_o\,\frac{\omega_{ie}}{\omega_s}\,\underline{U}_3(1-\cos\omega_s T)$$

$$+\,r_o\,\frac{\omega_{ie}^{\,2}}{\omega_s^{\,2}}\,\underline{U}_4(\omega_s T - \sin\omega_s T) + r_o\,\frac{\omega_{ie}}{\omega_s}\,\underline{U}_5\,\frac{1}{2}\,\omega_{ie}^{\,2}T^2]$$

Resetting the velocity integrator is equivalent to inserting a calculated step equal to:

$$\underline{\hat{\delta \dot{r}}}(T)^{a'} = \underline{\delta \dot{r}}(T)^{a'} - \underline{\varepsilon \dot{r}}(T)^{a'} \qquad (5.8c)$$

where the $\underline{\varepsilon \dot{r}}(T)^{a'}$ term is the inaccuracy in the calculated true velocity at t = T, including the effect of the wiggling of the vehicle.

Inserting the equations (5.8b, c) and (4.8a, b, c) into equation (5.8) and denoting:

$$t' = t - T$$

we get, for t > T or t' > 0:

$$\underline{\delta r}(t)^{a'} = \underline{\delta r}(0)^{a'} + \underline{\varepsilon r}(T)^{a'}\cos\omega_s t' + \frac{1}{\omega_s}\underline{\varepsilon \dot{r}}(T)^{a'}\sin\omega_s t'$$

$$+\,r_o\,[-\underline{E}_2 - \underline{E}_3\,\omega_{ie}T + \underline{U}_4\tfrac{1}{2}\,\omega_{ie}^{\,2}T^2](1-\cos\omega_s t')$$

$$+\,r_o\,\frac{\omega_{ie}}{\omega_s}\,[-\underline{E}_3 + \underline{U}_4\,\omega_{ie}T](\omega_s t' - \sin\omega_s t')$$

$$+\,r_o\,\frac{\omega_{ie}}{\omega_s}\,\underline{U}_4\,[\tfrac{1}{2}\,\omega_s^{\,2}t'^{\,2} - (1-\cos\omega_s t')]$$

$$+\,r_o\,\underline{U}_5\,\frac{1}{6}\,\omega_{ie}^{\,3}t^3$$

where the terms $r_o\,\frac{\omega_{ie}}{\omega_s}\,\underline{U}_5\,\frac{1}{2}\,\omega_{ie}^{\,2}T^2$ and $\underline{U}_5\,\frac{1}{6}\,\omega_{ie}^{\,3}T^3$ have been neglected because they give errors less than 100 feet for T < 20 minutes.

Propagated with $r_o\,(1-\cos\omega_s t')$, we have:

$$\underline{U}_2' = -\begin{bmatrix} \varepsilon_{2x} + \varepsilon_{3x}\,\omega_{ie}T \\ \varepsilon_{2y} + \varepsilon_{3y}\,\omega_{ie}T \\ \varepsilon_{2z} + \varepsilon_{3z}\,\omega_{ie}T \end{bmatrix} + \frac{1}{\omega_{ie}} \begin{bmatrix} 2\,\omega_{doz}\cos L_o + gMUY_y \\ -\omega_{ie}\psi_{\omega z}\sin L_o \cos L_o - gMUY_x \\ -2\omega_{dox}\cos L_o \end{bmatrix} \frac{1}{2}\,\omega_{ie}{}^2T^2$$

The last term $r_o\,\underline{U}_4\,\omega_{ie}{}^2T^2$ gives a maximum of 2,300 feet error for T = 20 minutes and t' = 42 minutes when the values in Table 3.1 are used.

Propagated with $r_o\,\frac{\omega_{ie}}{\omega_s}\,(\omega_s t' - \sin \omega_s t')$:

$$\underline{U}_3' = -\begin{bmatrix} \varepsilon_{3x} \\ \varepsilon_{3y} \\ \varepsilon_{3z} \end{bmatrix} + \frac{1}{\omega_{ie}} \begin{bmatrix} 2\omega_{doz}\cos L_o + gMUY_y \\ -\omega_{ie}\psi_{\omega z}\sin L_o \cos L_o - gMUY_x \\ -2\omega_{dox}\cos L_o \end{bmatrix} \omega_{ie}T \qquad (5.9b)$$

the last term here will give a 1.56 n.m. maximum error for t' = 84 minutes when T = 20 minutes and ω_{doz} = 10 meru.

The coefficient matrices for the last two time functions are given in (3.29d, e).

Comparing the position error expressed in equations (5.9a, b) with (5.4a, b) in paragraph 5.1, it is evident that we get a smaller error when realigning the platform after the compensation signals have been applied, provided that the random misalignment terms are small. The reason is that the misalignment caused by the gyro drift rates in the $\underline{U}_4$ matrix is not removed because this matrix cannot be estimated during the preflight test run.

5.3 Compensation without Realignment Using both Position and Accelerometer Error Data

At the end of the preflight test period, the indicated accelerometer error given by equation (4.4) is an almost direct measure of the misalignment, provided that adequate filtering of the accelerometer signals is performed and that possible compensation signals fed to point 2, Figure 5.1, are corrected for. By applying the corrected value of $\underline{\Delta f}^a$ at t = T at point 2, the total misalignment of the platform is ideally compensated for. From the accelerometer signal or from the position error data, the equivalent constant gyro drift can be determined and compensated for at point 4 in the same manner as described in paragraph 5.1.2 or $\underline{\hat{U}}_3$ is applied through integrators to point 2 as in paragraph 5.1.1. This last method will be used here. Similarly, the velocity and position integrators are also reset at

t = T.

The errors indicated by the accelerometers at t = T can be written as:

$$\underline{\Delta f}^a = g\{\underline{A}_1 + \underline{U}_3\ \omega_{ie}T + \underline{U}_4\ \frac{1}{2}\ \omega_{ie}{}^2T^2\}$$

The estimated value of $\underline{\Delta f}^a$ after filtering can be expressed as:

$$\underline{\Delta \hat{f}}(T)^a = g\{\underline{K}_1 + \underline{U}_3\ \omega_{ie}T + \underline{U}_4\ \frac{1}{2}\ \omega_{ie}{}^2T^2 + \underline{E}\} \tag{5.10}$$

where $\underline{E}$ is the difference between the filtered $\underline{A}_1$ and $\underline{K}_1$ matrices plus measurement uncertainties.

$$\underline{E} = \begin{bmatrix} (u)\ddot{r}'_x(T) + \varepsilon'_x \\ (u)\ddot{r}'_y\ (T) + \varepsilon'_y \\ \delta g/g + 3\frac{\delta h}{r_o} + (u)\ddot{r}'_z(T) + \varepsilon'_z \end{bmatrix} = \begin{bmatrix} \varepsilon_x \\ \varepsilon_y \\ \varepsilon_z \end{bmatrix} \tag{5.10b}$$

where $(u)r'_k(T)$, k = x, y, z is the residual of the filtered disturbance acceleration at t = T. At t = T, we can insert $\underline{\Delta \hat{f}}^a$ at point 2, Figure 5.1, $-g\ \omega_{ie}\hat{\underline{U}}_3$ through integrators to 2, $\underline{\delta \hat{r}}(T)^{a'}$ at 6, and $\underline{\delta \hat{\dot{r}}}(T)^a$ at 5.

An equation similar to (5.8) can then be derived from Figure 3.3 for a navigation run lasting less than one and a half hours.

$$\begin{aligned} \underline{\delta r}(t)^{a'} - \underline{\delta r}(0)^{a'} &= -\underline{\delta \hat{r}}(T)^{a'} \cos \omega_s(t-T) + \frac{1}{\omega_s}\ \underline{\delta V}(0)^{a'} \sin \omega_s t \\ &- \frac{1}{\omega_s}\ \underline{\delta \hat{\dot{r}}}(T)^{a'} \sin \omega_s(t-T) + r_o\ \underline{U}_2\ (1 - \cos \omega_s t) \\ &- r_o\ \underline{\Delta f}(T)^{a'}/g\ (1 - \cos \omega_s(t-T)) \\ &+ r_o\ \frac{\omega_{ie}}{\omega_s}\ \underline{U}_3(\omega_s t - \sin \omega_s t) \\ &- r_o\ \frac{\omega_{ie}}{\omega_s}\ \hat{\underline{U}}_3[\omega_s(t-T) - \sin \omega_s(t-T)] \\ &+ r_o\ \frac{\omega_{ie}{}^2}{\omega_s{}^2}\ \underline{U}_4[\frac{1}{2}\ \omega_s{}^2t^2 - (1 - \cos \omega_s t)] \\ &+ r_o\ \underline{U}_5\ \frac{1}{6}\ \omega_{ie}{}^3t^3 \end{aligned} \tag{5.11}$$

By inserting equation (5.8b) for $\underline{\delta \hat{r}}(T)^{a'}$, (5.8c) for $\underline{\delta \hat{\dot{r}}}(T)^{a'}$, (5.10) for $\underline{\Delta \hat{f}}(T)^a$, and (4.8c) for $\hat{\underline{U}}_3$ and denoting t' = t-T, equation (5.11) can be written for t > T as:

$$\underline{\delta r}(t)^{a'} = (\underline{\delta r}(0)^{a'} + \underline{\varepsilon r}(T)^{a'}) \cos \omega_s t' + \frac{1}{\omega_s}\underline{\dot{\varepsilon r}}(T) \sin \omega_s t'$$

$$- r_o \underline{E} (1 - \cos \omega_s t') + r_o \frac{\omega_{ie}}{\omega_s} [-\underline{E}_3 + \underline{U}_4 \omega_{ie} T]$$

$$(\omega_s t' - \sin \omega_s t') + r_o \frac{\omega_{ie}^2}{\omega_s^2} \underline{U}_4 [\frac{1}{2} \omega_s^2 t'^2 - (1 - \cos \omega_s t')]$$

$$+ r_o \underline{U}_5 \frac{1}{6} \omega_{ie}^3 t^3 \qquad (5.11b)$$

where the following terms have been omitted because they give a negligible contribution:

$$- r_o \frac{\omega_{ie}}{\omega_s} \underline{U}_5 \frac{1}{2} \omega_{ie}^2 T^2 \sin \omega_s t',$$

$$- r_o \underline{U}_5 \frac{1}{6} \omega_{ie}^3 T^3 (1 - \cos \omega_s t'), \text{ and}$$

$$- r_o \underline{U}_5 \frac{1}{6} \omega_{ie}^3 T^3$$

Comparing equation (5.11b) with (5.9) the improvement obtained is a reduction of the coefficient of the $(1 - \cos \omega_s t')$ term because the compensation of the misalignment error can be made more accurate using the accelerometer data.

Comparing equation (5.11b) with (5.4), where alignment was used after compensation, a reduction in the misalignment error could be obtained using the accelerometer data and not realigning the system, but the equivalent drift terms propagated with $(\omega_s t - \sin \omega_s t)$ have increased by the amount of $\underline{U}_4 \omega_{ie} T$. The matrix cannot be determined during the preflight test run. Therefore compensation cannot be generated, and the only way to reduce the effect of these drift rates is to realign the system.

One way of mechanizing this system is shown in Figure 5.2. Here T is the length of the preflight test run.

$$\underline{\Delta \hat{f}}^{a'}(T) = \underline{K}_1 + \underline{U}_3 \omega_{ie} T + E$$

$$\underline{\Delta \hat{f}}^{a'} = \underline{U}_3 \omega_{ie} + \underline{E}' \qquad (5.12)$$

where the $\underline{U}_4$ term in equation (4.4) has been neglected.

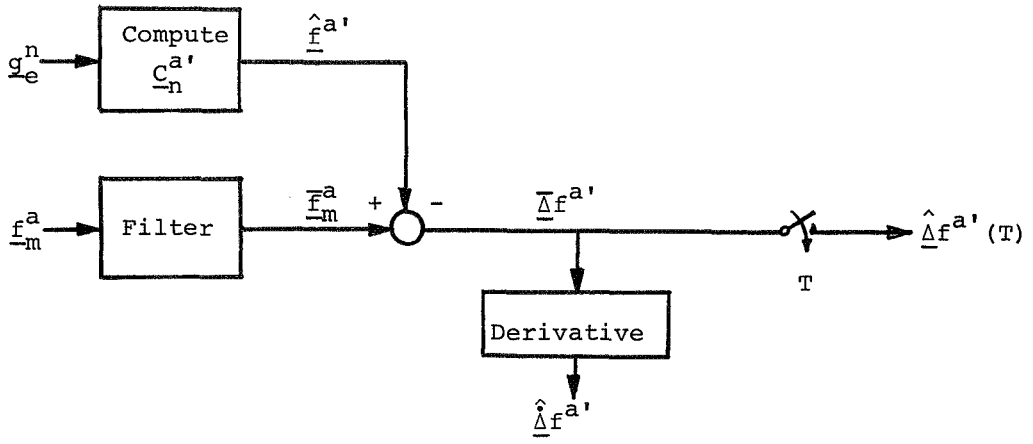

Figure 5.2
Possible Mechanization of Compensation Signals

The filter box can consist of a counter counting the ΔV pulses from the accelerometers for a time interval τ, holding this value and resetting the counter, and then repeating the cycle. Because the bandwidth of the information and the disturbances is widely separated, adequate filtering can be obtained by letting τ be several seconds. The value of $\hat{\underline{f}}^{a'}$ has to be computed every τ seconds. Given τ, g, and L_o this computation can be done prior to the test run. The value of the filtered acceleration error, $\overline{\underline{\Delta f}}^{a'}$, at t = T, denoted $\hat{\underline{\Delta f}}^{a'}(T)$, is fed to point 2, Figure 5.1.

From the $\underline{\Delta f}^{a'}$ value one can, by various techniques, derive an estimate of the t dependent term by neglecting the higher order terms. This estimate of $\hat{\underline{\dot{\Delta f}}}^{a'}$ is then fed via integrators to Figure 5.1 after proper scaling. The effect of neglecting the term $\underline{U}_4 \frac{1}{2} \omega_{ie}{}^2 t^2$ in the expression for the acceleration error will have the following effect on $\underline{\dot{\Delta f}}^{a'}$:

$$\underline{\dot{\Delta f}}^{a'} = \underline{U}_3 \omega_{ie} + \underline{U}_4 \omega_{ie}{}^2 t$$

Taking the mean value of this expression for the test interval, we get:

$$\overline{\underline{\dot{\Delta f}}}^{a'} = \omega_{ie} [\underline{U}_3 + \underline{U}_4 \frac{1}{2} \omega_{ie} T]$$

Using the maximum uncertainties given in Table 3.1, this last term gives only 0.5×10^{-3} for T = 15 minutes, compared with 10×10^{-3} for the first term. Thus the assumption made by neglecting higher order

time functions in (5.10) should be valid.

It is also necessary to compute $\underline{\dot{r}}^i(T)$ and $\underline{r}^i(T)$ to reset the two integrators in the navigation computer. These two values can be computed prior to the test run and depend only upon L_o, provided that T is fixed.

5.4 The Use of Data from the Alignment Phase

The signals which could be made available during the alignment phase are the accelerometer signals and the command signals to the gyro torquers. It is only necessary to study these signals under steady state conditions.

5.4.1 The Gyro Torquer Command Signals

Using equations (2.3a, b) we can write:

$$\underline{\omega}^a_{ia} = \underline{\omega}^a_{CMD} + \underline{\omega}^a_{do} = \underline{\omega}^a_c + \underline{\omega}^n_{in} + \underline{\omega}^a_{do}$$

$$\underline{\omega}^a_{ia} = \underline{C}^a_n \, \underline{\omega}^n_{in} + \underline{\omega}^a_{na}$$

where $\underline{\omega}^a_c$ denotes the signals coming from the alignment electronics and $\underline{\omega}^n_{in}$ denotes the constant earth rate compensation signals.

Rewriting the equations above we get:

$$\underline{\omega}^a_c = (\underline{C}^a_n - \underline{I})\underline{\omega}^n_{in} + \underline{\omega}^a_{na} - \underline{\omega}^a_{do} \tag{5.13}$$

Dealing only with the steady state, the $\underline{\omega}^a_{na}$ matrix, given by (2.5), can be set equal to zero. Inserting equations (2.4), (2.6), and (2.1) into (5.13) yields:

$$\underline{\omega}^a_c = \begin{bmatrix} \omega_{cx} \\ \omega_{cy} \\ \omega_{cz} \end{bmatrix} = \omega_{ie} \begin{bmatrix} C_y \sin L_o \\ -C_z \cos L_o - C_x \sin L_o \\ C_y \cos Lo \end{bmatrix} - \begin{bmatrix} \omega_{dox} \\ \omega_{doy} \\ \omega_{doz} \end{bmatrix} \tag{5.14}$$

The command rates consist of fixed gyro drift rates and components of the earth rate due to misalignment, factors which are not compensated for. Referring to the values listed in Table 3.1, the gyro drift rates are expected to be the predominant terms for system 1. This justifies the following equation for gyro drift estimates:

$$\hat{\underline{\omega}}^a_{do(1)} = -\underline{\omega}^a_c - \omega_{ie}\underline{E}_4 \tag{5.15}$$

where

$$\underline{E}_4 = \{\varepsilon_{4x}, \varepsilon_{4y}, \varepsilon_{4z}\} \tag{5.15a}$$

are the errors in the estimates caused by gyro torquer uncertainties, measurement uncertainties, and errors caused by limit cycles or transients not taken into consideration in the steady state analysis.

By using equations (2.18a, c) for system 2, equation (5.14) becomes:

$$\underline{\omega}^a_{C(2)} = \omega_{ie} \begin{bmatrix} C_y \sin L_o \\ -\zeta_{cz} \cos L_o \\ C_y \cos L_o \end{bmatrix} - \begin{bmatrix} \omega_{dox} \\ 0 \\ \omega_{doz} \end{bmatrix} \tag{5.15b}$$

The best estimate of the gyro drift rates will then be:

$$\underline{\hat{\omega}}^a_{do(2)} = -\begin{bmatrix} \omega_{cx} \\ 0 \\ \omega_{cz} \end{bmatrix} - \omega_{ie} \begin{bmatrix} \varepsilon_{4x} \\ 0 \\ \varepsilon_{4z} \end{bmatrix} \tag{5.15c}$$

If the drift estimates are derived just before the alignment phase is finished and the compensation signals applied at point 4, Figure 5.1, at t = 0, we get the following constant drift rates valid for the navigation mode:

$$\underline{\omega}'^a_{do} = \underline{\omega}^a_{do} - \underline{\hat{\omega}}^a_{do} \tag{5.16}$$

or

$$\underline{\omega}'^a_{do} = \omega_{ie} \begin{bmatrix} C_y \sin L_o + \varepsilon_{4x} \\ 0 \\ C_y \cos L_o + \varepsilon_{4z} \end{bmatrix} + \omega_{ie} \underbrace{\begin{bmatrix} 0 \\ -C_z \cos L_o - C_x \sin L_o + \varepsilon_{4y} \\ 0 \end{bmatrix}}_{(1)} + \underbrace{\begin{bmatrix} 0 \\ \omega_{doy} \\ 0 \end{bmatrix}}_{(2)} \tag{5.16a}$$

where

$\underline{C}^a = \{C_x, C_y, C_z\}$ is given by equation (2.11) for system 1 and (2.16) for system 2

The effect of this compensation of the error propagation during a maximum one and a half hour run can be found from equations (3.29a, b, c, d, e) by replacing $\underline{\omega}^a_{do}$ with equation (5.16a). This gives the following result:

$\underline{U}_2$ propagating with r_o (1 - cos $\omega_s t$) remains unchanged.

The uncertainty matrix propagating with $r_o \frac{\omega_{ie}}{\omega_s}$ ($\omega_s t$ - sin $\omega_s t$) is changed.

By using equations (3.31) and (5.16a) we get:

$$\underline{U}_3' = \begin{bmatrix} C'_z \\ 0 \\ -C'_x \end{bmatrix} \cos L_o + \frac{1}{\omega_{ie}} \begin{bmatrix} \omega'_{doy} \\ -\omega'_{dox} \\ 0 \end{bmatrix} \tag{5.21}$$

$$\underline{U}_3' = \begin{bmatrix} 0 \\ -C_y \sin L_o - \varepsilon_{4x} \\ -C'_x \cos L_o \end{bmatrix} + \begin{bmatrix} \zeta_{rz} \cos L_o - C_x \sin L_o + \varepsilon_{4y} \\ 0 \\ 0 \end{bmatrix}_{(1)} + \begin{bmatrix} C'_z \cos L_o \frac{\omega_{doy}}{\omega_{ie}} \\ 0 \\ 0 \end{bmatrix}_{(2)}$$

where $\underline{C}'^{a} = \underline{C}^{a} + \underline{\zeta}_r^{a}$ was used. Inserting equation (2.18a) and (2.18c) and making the same simplifications as were done for equation (3.29c), we get:

$$\underline{U}_3' = \begin{bmatrix} -\delta f_y/g \sin L_o \\ (\delta f_x/g - \zeta_{cy}) \sin L_o - \varepsilon_{4x} \\ -(\delta f_y/g + \zeta_x) \cos L_o \end{bmatrix} + \begin{bmatrix} \zeta_{rz} \cos L_o - \zeta_{cx} \sin L_o + \varepsilon_{4y} \\ 0 \\ 0 \end{bmatrix}_{(1)}$$

$$+ \begin{bmatrix} \zeta_z \cos L_o - \zeta_x \sin L_o \\ 0 \\ 0 \end{bmatrix}_{(2)} \tag{5.17a}$$

The uncertainty matrix propagated with $r_o \frac{\omega_{ie}^2}{\omega_s^2} [\frac{1}{2} \omega_s^2 t^2 - (1 - \cos \omega_s t)]$ can be found by equations (3.29d), (5.16a), and (2.18a, c):

$$\underline{U}_4' = \frac{2 \cos L_o}{\omega_{ie}} \begin{bmatrix} \omega'_{doz} \\ 0 \\ -\omega'_{dox} \end{bmatrix} + \frac{g}{\omega_{ie}} \begin{bmatrix} MUY_y \\ -MUY_x \\ 0 \end{bmatrix} + \begin{bmatrix} 0 \\ \frac{\omega_{doy}}{\omega_{ie}} \sin L_o \\ 0 \end{bmatrix}_{(2)}$$

$$\underline{U}_4' = 2\cos L_o \begin{bmatrix} C_y \cos L_o + \varepsilon_{4z} \\ 0 \\ -C_y \sin L_o - \varepsilon_{4x} \end{bmatrix} + \frac{g}{\omega_{ie}} \begin{bmatrix} MUY_y \\ -MUY_x \\ 0 \end{bmatrix} + \begin{bmatrix} 0 \\ \frac{\omega_{doy}}{\omega_{ie}} \sin L_o \\ 0 \end{bmatrix}_{(2)} \quad (2)$$

or finally:

$$\underline{U}_4' = 2\cos L_o \begin{bmatrix} (-\delta f_x/g+\zeta_{cy})\cos L_o+\varepsilon_{4z} \\ 0 \\ -(-\delta f_x/g+\zeta_{cy})\cos L_o-\varepsilon_{4x} \end{bmatrix} + \frac{g}{\omega_{ie}} \begin{bmatrix} MUY_y \\ -MUY_x \\ 0 \end{bmatrix} + \begin{bmatrix} 0 \\ \frac{\omega_{doy}}{\omega_{ie}} \sin L_o \\ 0 \end{bmatrix}_{(2)} \quad (2)$$

(5.17b)

The uncertainties propagating with $r_o \frac{1}{6} \omega_{ie}{}^3 t^3$ can be found by using (3.29e) together with (5.16a) and (2.18a, c):

$$\underline{U}_5' = \frac{3\cos L_o}{\omega_{ie}} \begin{bmatrix} -\omega'_{doy} \cos L_o - \frac{1}{3} \omega_{ie} \psi_{\omega z} + gMUY_z \\ \omega'_{dox} \cos L_o - \omega'_{doz} \sin L_o \\ \omega'_{doy} \sin L_o - gMUY_x \end{bmatrix}$$

$$\underline{U}_5' = \frac{3g \cos L_o}{\omega_{ie}} \begin{bmatrix} MUY_z \\ 0 \\ -MUY_x \end{bmatrix} + \frac{1}{\omega_{ie}} \begin{bmatrix} -\omega_{doy}(3\cos^2 L-1) \\ 0 \\ 3\omega_{doy}\cos L_o \sin L_o \end{bmatrix}_{(2)} \quad (5.17c)$$

where neglecting terms giving less than 260 feet during a one and a half hour run when values given in Table 3.1 are used.

Comparing $\underline{U}_3'$, $\underline{U}_4'$, and $\underline{U}_5'$ with $\underline{U}_3$, $\underline{U}_4$, and $\underline{U}_5$ given by equations (3.29c, d, e), it is evident that a decrease in the uncertainty matrices has been obtained. The reason is that C_k, k = x, y, z for system 1, k = x, y for system 2, are approximately one tenth of ω_{doy}/ω_{ie} when the values of Table 3.1 are used. The greatest relative improvement has been obtained for the $\underline{U}_3'$ matrix. The x and y components of this matrix can be expected to be reduced by a factor of 10 provided that $\underline{E}_4$ is less than 10^{-3}. The relative improvement of the $\underline{U}_4'$ and $\underline{U}_5'$ matrices compared to $\underline{U}_4$ and $\underline{U}_5$ is less because the mass unbalance terms remain unchanged, but the effect of the constant gyro drift rates has been reduced.

If (5.15) had been used to estimate the y gyro drift rate for system 2, the expression for $\underline{U}_{3(2)}'$ would be the same as for $\underline{U}_{3(1)}'$.

An improvement would then be obtained if the ε_{4y} uncertainty is much less than ζ_{cz} or ζ_{rx}. This would be the best way of using the information gained by measuring the y gyro command signal. The other uncertainty matrices would remain unchanged by using ω_{cy} as a compensation signal.

Another possible scheme could be to derive the drift estimates and make the compensation and then continue the alignment until the steady state is reached. It should then be possible to reduce the misalignment due to gyro drift in system 1 and thereby reduce the $\psi_{\omega x}$ and $\psi_{\omega y}$ terms in the expression for $\underline{U}_2$, equation (3.29b). By recording the gyro command signals when the alignment is finished, one could check that the correct compensation signals had been applied. This scheme would give an increased alignment time, and the benefit obtained by reducing the misalignment error caused by gyro drift could also have been accomplished by increasing the gains in the alignment loops. Because the gyro command signals do not give any information about the y gyro drift rate for system 2, and because it was assumed that the loop gains in the x and y channels were high, the elongated alignment would not give us any advantages for system 2.

5.4.2 The Accelerometer Outputs at the End of the Alignment Phase

When the alignment phase has reached the steady state, we can express the outputs from the accelerometers by using equations (2.17) and (3.14):

$$\begin{aligned} \underline{f}_m^a &= (\underline{I} + \underline{A}^a)(\underline{I} + \underline{\psi}^a)\underline{f}^n + \underline{\delta f}^a \\ \underline{f}_m^a &\simeq \underline{f}^n + (\underline{A}^a + \underline{\psi}^a)\underline{f}^n + \underline{\delta f}^a \end{aligned} \tag{5.18}$$

Inserting the equations (2.8), (2.18b) and (2.2) yields:

$$\underline{f}_m^a = g \begin{bmatrix} \psi_{\omega y} + \zeta'_y \\ -\psi_{\omega x} - \zeta'_x \\ \delta f_x/g - (1+a_z) \end{bmatrix} + \begin{bmatrix} (u)\ddot{r}_x \\ (u)\ddot{r}_y \\ (u)\ddot{r}_z \end{bmatrix} \tag{5.18a}$$

By filtering the accelerometer signals and subtracting the gravity from the z accelerometer signal, we get

$$\overline{\underline{\Delta f}}_m^a = g \begin{bmatrix} \psi_{\omega y} + \zeta'_y + \varepsilon_{5x} \\ -\psi_{\omega x} - \zeta'_x + \varepsilon_{5y} \\ \psi_{fx}/g - a_z + \delta g + \varepsilon_{5z} \end{bmatrix} \tag{5.19}$$

The misalignment terms, ζ'_k, k = x, y include only the ζ_{ck} terms, caused by alignment electronics offsets, and "slowly varying" limit cycles and transients which are not filtered out. The misalignment term described in point c) in connection with equation (2.17d) is, of course, not included.

The error terms, ε_{5k}, k = x, y, z, comprise uncertainties in measuring $\underline{\Delta f}^a$ together with improper filtering of (u)$\underline{\ddot{r}}$ terms.

Applying (5.19) as a compensation signal at point 2, Figure 5.1, when the system is switched to the navigation mode, we get the following error propagation during a one and a half hour run from equation (3.29):

Propagated with $r_o(1 - \cos \omega_s t)$:

$$\underline{U}'_2 = \begin{bmatrix} \partial f_x/g + \Delta\zeta_y + \varepsilon_{5x} \\ \partial f_y/g - \Delta\zeta_x + \varepsilon_{5y} \\ \delta g - 2\frac{\delta h}{r_o} + \varepsilon_{5z} \end{bmatrix} \qquad (5.20)$$

where $\Delta\zeta_k = \zeta_k - \zeta'_k$, k = x, y, z

The other uncertainty matrices $\underline{U}_3$, $\underline{U}_4$, and $\underline{U}_5$ remain unchanged.

The advantage of this method in determining the misalignment is that a minimum of computation is required because the accelerometer outputs can be used without any coordinate transformations.

The disadvantage is, of course, that the changes in the bias levels and in the platform attitude due to the switching of the system to the navigation frame are not detected. Because these changes are caused by imperfections in the electronics and not in the inertial components, efforts should be made in reducing these effects instead of building sophisticated test equipment in order to detect the changes in a preflight test run.

When using pulse restrained accelerometers where the outputs are in the form of velocity increments, we get the same requirements on the length of the test as depicted in paragraph 4.3. That means that a test time in excess of ten minutes is necessary in order to detect misalignment terms down to 20 μrad corresponding to a maximum position error of 820 feet (Refer to Figure 3.2).

The information derived from the alignment phase, equations (5.14) and (5.19), together with the information gained from the preflight test run, equations (4.8b, c), is still not adequate to determine all the I.N.S. uncertainties. The only additional information gained from the alignment phase is the z gyro drift rate.

5.4.3 Position Error Propagation Using Only Data from the Alignment Phase

By using both the accelerometer data and the gyro command signals, the uncertainty matrices valid for a maximum one and a half hour run are given by equations (5.20), (5.17a, b, c) for $\underline{U}_2'$, $\underline{U}_3'$, $\underline{U}_4'$, and $\underline{U}_5'$ respectively. The error propagation is given by equation (3.29) when $\underline{U}_i$ is replaced by $\underline{U}_i'$, i = 2, 3, 4, 5. The effects of the uncompensated uncertainty terms can be found from Figure 3.2. For convenience, the major terms are listed in table 5.2.

Item	Units	Position Error		
		42 min	63 min	84 min
$\delta V(0)_k$, k = x, y, z	ft/ft/s	0	800	0
∂f_k, k = x, y, δg	ft/μg	42	21	0
$\Delta\zeta_k$, k = x, y	ft/μrad	42	21	0
δf_k, k = x, y	ft/mg	2720	4950	5450
ζ_k, ζ_{ck}, ζ_{rk}, k = x, y, z	ft/mrad	2720	4950	5450
ε_{4x}, $\varepsilon_{4y(1)}$	ft/10^{-4}	384	698	767
$gMUY_k$, k = x, y	ft/meru	210	688	1404
$\omega_{doy(2)}$	ft/meru	148	488	984
ε_{4z}	ft/10^{-4}	30	98	194
$gMUY_z$	ft/meru	46	151	360

L_o = 45° 1 mrad = 3.44 min 1 rad ≈ 0.2 sec

Table 5.2
Effect of Uncompensated Uncertainties Using Alignment Data

As can be seen from the above table, the uncompensated gyro drift rates will give the most significant error terms. Comparing this table with table 5.1, derived for the case where a preflight test run with a subsequent realignment was used, it is clear that many of the major error sources are the same.

6. CONCLUSION

The propagation of the position error valid for at least one and a half hours was derived for navigation on a stationary base. For an actual flight with low speed aircraft, only minor changes are expected in the equation for the error propagation. Thus the conclusions derived should also be valid for that case, provided that the alignment and the test run are made on a stationary base. The

equivalent block diagram valid for this error equation is shown in Figure 3.3. The I.N.S. uncertainties enter the Schuler tuned loop in the following way:

(a)	With no integration:	Platform misalignment and bias shift
(b)	With one integration:	Fixed gyro drift rates and misalignment
(c)	With two integrations:	Acceleration-sensitive gyro drift rates for the y gyro, together with cross coupled fixed gyro drifts
(d)	With three integrations:	Acceleration-sensitive gyro drift rates and cross coupling of the fixed gyro drifts

From the preflight test run lasting less than 20 minutes, only the error inputs mentioned in (a) and (b) can be detected using maximum values of the uncertainties given in Table 3.1. As explained in paragraph 4.3, the test run should last at least 10 minutes, preferably 15 minutes, in order to determine the fixed gyro drift rates when 0.1 ft/sec velocity increments from the accelerometers are assumed. Extending the duration of the test run to 20 minutes will not give reliable estimates of the acceleration-sensitive gyro drift terms using a simple curve-fitting method.

The I.N.S. uncertainties can be estimated using properly filtered accelerometer data or using the position data. For a test run lasting less than 15 minutes, the position error is essentially the double integral of the acceleration error data.

As explained in Chapter 4, it is not possible to determine all the major I.N.S. uncertainties from a simple preflight test run. By also using the information gained from the alignment phase, we still do not have enough data to determine all the uncertainties separately.

Five different methods of applying the estimated data are described in Chapter 5. In paragraph 5.1 a realignment of the platform is performed after the compensation signals have been applied. A combination of the methods used in paragraphs 5.1.1 and 5.1.2 seems to give the best results provided that the change in the uncertainties from alignment to alignment is small. These methods require a considerable amount of computation, and the realignment is rather time consuming.

In paragraphs 5.2 and 5.3 the uncertainties are compensated for without a subsequent realignment using position data and filtered accelerometer data, respectively. The last method seems to be the most accurate and requires somewhat less computation.

In paragraph 5.4 a method using only data from the alignment phase is described. This method requires a minimum of computation and therefore deserves serious consideration. This scheme fails, however, to detect changes in the I.N.S. uncertainties when the system is switched from the alignment phase to the navigation phase.

The effect of not compensating for the acceleration-sensitive gyro drift terms can give as much as 2.3 n.m. position error when exposed to a 10 meru/g gyro drift for a one and a half hour run. The effects of initial latitude and altitude errors and deflection of the vertical (on a stationary base) have all proven to be negligible compared to the other error sources given in Table 3.1.

It seems from this work that a space stabilized IMU is not especially suitable when a preflight test run is necessary in order to determine the I.N.S. uncertainties due to the amount of computation involved. Another argument against using a space stabilized platform is the effect of the acceleration-sensitive gyro drift rates which could have been neglected when using a local vertical system.

Reference

Britting, K.R., "Analysis of Space Stabilized Inertial Navigation Systems," M.I.T. RE-35, Experimental Astronomy Laboratory, November, 1968.